Jérémie Janin
Class 2016-2019

Industrial tutor: Dr. Bernd Dressel
Academic tutor: Dr. Sylvain Serra

INTERNSHIP REPORT

ENGENEERING MASTER'S DEGREE

STUDY: FSI coupled CFD simulation on HTP design

ENSGTI
ÉCOLE D'INGÉNIEURS

Confidential Report

Acknowledgments

First of all, I would like to thank all the staff at Framatome in the fuel mechanics department for their integrity, support, availability, eagerness and willingness to answer any questions.

I would like to thank in particular;

- Dr. Bernd Dressel, my tutor throughout this internship, for his personal investment, assistance and the time he as dedicated to me. He taught me a lot about CFD and mechanical behavior of fuel assemblies. I was trusted in the tasks he assigned me and he gave me a sound understanding of the behavior of PWR core in accidental situation.
- Dr. Markus Wicklein, team manager, for welcoming me and answering all my questions.
- Dr. Hidajet Hadzic, CFD expert, for his time and his cooperation in explaining me particular features of STAR-CCM+.

TABLE OF CONTENTS

LIST OF TABLES

LIST OF FIGURES

ABBREVIATIONS

CFD	computational fluid dynamics
FA	fuel assembly
FR	fuel rod
FSI	fluid structure interaction
GT	guide tube
RANS	Reynolds averaged Navier-Stokes
SG	spacer grid

REFERENCES

[1] T. J.R. Hughes
The Finite Element Method – Linear Static and Dynamic Finite Element Analysis
Prentice-Hall, Inc., New Jersey, 1987

[2] George A. Papagiannopoulos, George D. Hatzigeorgiou
On the use of the half-power bandwidth method to estimate damping in building structures
Soil Dynamics and Earthquake Engineering journal, 2011

[3] B. Dreßel
CFD FSI simulations of the dynamic behavior of an HTP 8x8 fuel bundle under axial flow
Technical Report FS1-0024423 Rev. 1.0, dated 2015-12-17

1. INTRODUCTION

The present report summarizes the calculation of dynamic pluck tests and sinus-sweep tests for an HTP 15x15 in stagnant water and the recalculation of dynamic pluck tests for an HTP 8x8 design under axial flow as well. This kind of simulation is characterized by strong FSI effects and therefore an FSI coupled CFD implementation is realized with the commercial software STAR-CCM+. When possible, these simulations will be benchmarked with experimental data. Indeed, Framatome carries out tests at the PETER loop in Erlangen (Pressurized Water Reactor Fuel Assembly Tests).

The main goal of this study is to determine damping values and eigenfrequency. These values are necessary in order to predict the reaction of FA under accident (i.e. seismic events).

The structure of the report is as follows:

In section 2, Framatome will be presented.

In section 3, the mechanical model is described. The latter applies for both HTP 15x15 model and HTP 8x8. We explain here how the beam model is implemented.

Since there is no difference regarding the methodology between the two models we also explain how the FSI is applied in section 4. The CFD simulations use a strong coupling between the Fortran user coded dynamic beam equations and the commercial CFD software STAR-CCM+

Section 5 shows results concerning the HTP 15x15 design in stagnant water. First of all we describe the CFD model used for simulations and then present the pluck test results as well as results from sinus-sweep tests. After discussion of these results we study the impact of confinement effect. In order to certify that the used HTP 15x15 model is reliable, a sensitivity study has been performed.

In section 6, we present results regarding the HTP 8x8 design under axial flow (5m/s). We first introduce the used model and then describe the simulation methodology.

The report ends with a summary and conclusion in section 7.

2. HOST COMPANY

2.1. GENERAL INFORMATION

Company name: FRAMATOME GmbH
VAT id number: DE 310 766 750
Managing Director: Carsten Haferkamp
Address: Framatome GmbH, Paul-Gossen-Straße 100, 91052 Erlangen, Germany
Telephone: +49 9131 900 0
Email: kontakt.deutschland@framatome.com
Website: www.framatome.com

The share capital social of Framatome is owned 75.5 % by the EDF French group, 19.5 % by Mitsubishi and 5 % by Assystem. With an order book of 15 billion Euros and presence in 18 countries, Framatome is leader throughout the world in nuclear industry.

The company has 14000 employees and worked on 25 power plant a crossed the world.

2.2. HISTORY

Since its foundation in 1958, Framatome has been manufacturing Pressurized Water Reactor (PWR) and Boiling Water Reactor (BWR). In 2006, Framatome changes its name to AREVA NP before changing again to Framatome in 2018. Framatome is involved in the design, the manufacturing of nuclear power plants and associated services, components, fuel and instrumentation and control

systems. Framatome is headquartered in Paris (France) with main subsidiaries in the United States (Framatome Inc.) and Germany (Framatome GmbH). I have worked in Framatome GmbH company. This subsidiary has three mains location in Germany: Offenbach, Erlangen and Karlstein. My office and activities were in Erlangen. I have worked in the Fuel Mechanics department with the CFD expert team.

3. MECHANICAL MODEL

In order to capture the FA dynamics, the equation of motion is integrated for the beam displacement / rotation vector $\underline{u} = (u_i, \varphi_i)$.

$$M_{st}.\ddot{\underline{u}} + D_{st}.\dot{\underline{u}} + K_{st}.\underline{u} = \underline{F_{fl}} + \underline{F_{ext}} \tag{1}$$

In the latter equation M_{st}, D_{st} and K_{st} denote the structural mass, damping and stiffness matrix. $\underline{F_{fl}}$ and $\underline{F_{ext}}$ are respectively the fluid forces and external forces, e.g. inertia loads in sinus-sweep tests.

Concerning the discretization approach, we choose to solve the FA structural dynamics with the Finite Element representation. The beam nodes are distributed along the axial position of the FA (see Figure 4 and Figure 19). There is a beam node at each spacer grid and four beam nodes between two SG. Two beam nodes are located near the top and bottom part.

Based on this discretization, the structural stiffness matrix

$$K_{st} = \sum k_i \qquad \text{(for } i = 1, \dots, nb \text{ where } nb \text{ is the number of beam nodes)}$$

is calculated from the stiffness matrix

$$k_i = \mathrm{EI} \times \begin{pmatrix} \frac{12}{l_i^3} & \frac{6}{l_i^2} & -\frac{12}{l_i^3} & \frac{6}{l_i^2} \\ \frac{6}{l_i^2} & \frac{4}{l_i} & -\frac{6}{l_i^2} & \frac{2}{l_i} \\ -\frac{12}{l_i^3} & -\frac{6}{l_i^2} & \frac{12}{l_i^3} & -\frac{6}{l_i^2} \\ \frac{6}{l_i^2} & \frac{2}{l_i} & -\frac{6}{l_i^2} & \frac{4}{l_i} \end{pmatrix} \tag{2}$$

of the individual beam elements $i = 1, \dots, nb - 1$ with length $l_i = z_i - z_{i-1}$

Concerning the diagonal mass matrix M_{st}, the displacement and rotation nodal masses are calculated with the following equations:

$$m_i = \frac{m_{FA}.\bar{l}_i}{l_{FA}} \tag{3}$$

$$\theta_i = \frac{m_i}{12}.\left(\bar{l}_i^2 + X^2 + 12.\Delta l_i^2\right) \quad (4)$$

With beam length and distance from gravity center as follow:

$$\bar{l}_i = \frac{(l_i + l_{i+1})}{2} \quad (5)$$

$$\Delta l_i = \frac{\left(\bar{l}_i - l_i\right)}{2} \quad (7)$$

The structural damping matrix D_{st} is implemented as Rayleigh damping:

$$D_{st} = \alpha.K_{st} + 2\beta.M_{st} \quad (8)$$

Where α and β are extracted from plug test excitation in air. These values will be given in Section 4 and Section 5 for the different FA design.

4. CFD – FSI IMPLEMENTATION

In order to deal with large CFD model (100-400 M fluid cells) a highly efficient FSI model is needed to benchmark results with PETER loop experiments. It has already been proven that commercial code as ABAQUS are not suitable for this kind of design analysis. The one which has been used for this study is the so called BALKEN Fortran code. The latter is composed of several subroutine (interpolation, solution of linear equation, …) but we will focus on 4 of them to well understand how the USERcoding works. As soon as we implement the USERcode in the STAR-CCM+ the main program BALKEN become a subroutine. The Displacement solution of the equation of motion is given by the *balken* and the motion is applied to the fluid domain by the *mover* subroutine. By using the *regsplit* subroutine the FA is split in several area. And *fcalci*, is used to calculate the force on these area at every inner iteration.

All the subroutines are compiled as object files in a shared library (.so) and then linked to CFD solver. An interface subroutine which contain all the function that the user wants to integrate in the CFD software is needed. Moreover, STAR-CCM+ gives an easy handling, one need to download his library in Tools\User Code tree node and then it has access to functions that were defined in the interface.

The mechanical beam approach requires a calculation of the fluid forces on axial segments of the FA structural surfaces by the CFD solver in every inner iteration (cf. Figure 1). The most efficient and flexible way to perform the force integration in the user routine *fcalc* is to index the boundary faces allocated to a node of the FA beam with an integer number.

The *resplit* subroutine is used for this purpose to split the FA by the number of nodes. As explained in Section 2, the HTP 15x15 design (8 SG) contains 40 nodes but we remove the first and last nodes which correspond to constrained nodes, so it has 38 nodes. In the same manner HTP 8x8 (10 SG) design will contain 48 nodes. Figure 2 shows a visualization of the force region indices determined by the *regplit* subroutine for the HTP 15x15 design.

In the *fcalci* subroutine the hydraulic force is calculated as

$$F_h = p.x^2 + wss.\sqrt{(x^2 + y^2 + z^2)} \quad (9)$$

where p, wss, x, y, z denote respectively the scalar pressure, the WallShearStress in x direction and the x,y,z components for a boundary face delivered by STAR-CCM+.

This force is calculated and summed all over the partition into a variable f_x. Then the mass inertia forces F0 is added to this force in the vector F2 which is the return of the *fcalci* subroutine and transmit to the *mover* subroutine (see Annex)

At the beginning of the simulation, the mover subroutine read initial displacement from a text file (*mnodes.dat*), it calculates scaling factors in bypass area according to the formula:

$$x < (xwall1 + byp1) : f_{FA}(x) = \frac{x - xwall1}{byp1} \quad (10)$$

$$x > (xwall2 - byp2) : f_{FA}(x) = \frac{xwall2 - x}{byp2} \quad (11)$$

$$(xwall2 - byp2) < x < (xwall1 - byp1) : f_{FA}(x) = 1 \quad (12)$$

xwall1, xwall2, byp1 and byp2 are respectively the position left and right of the domain´s walls and the dimension of the left and right bypass. The scaling factor are defined for each fluid vortex according to its x coordinate in the undeformed CFD geometry. The displacement of each vertex in the FSI coupled CFD simulations is determined as linear combination of the FA deformation $x_{FA}(z)$ in x direction and the constant scaling factors f_{FA}. For this purpose, the displacement solution at the axial beam discretization points is interpolated by a spline algorithm.

During one time step the Newmark algorithm [1] is called at every inner iteration to solve the equation of motion and deliver the new displacement. To ensure convergence, the number of inner iterations of the fluid solver should be chosen sufficiently high in its default setting (e.g 30 for HTP 15x15 and 20 for 8x8).

Although the implementation between Fortran code and STAR-CCM+ is user friendly, one needs to be careful when starting simulations. Indeed, a few things need to be done before starting the simulation to avoid divergence of the solution due to the grid flux equation. We had to deal with diverging simulations after few iteration steps when the *mnodes.dat* is read at the beginning of the simulation. In-between one iteration the FA is moving from 0 mm to 5 A_0 mm in the case of the 5 A_0 mm pluck test amplitude. Therefore, a lot of mass water is displaced and creates local high velocity which is causing the simulation to diverge. An easy way to avoid this kind of issue is to initialize the position of the FA before starting simulation. This is done by activing Initial Displacement under the Region/Fluid/Physics Conditions node in STAR-CCM+ and also zero grid flux under Solver/User Defined Vertex Motion node. Then, one can initialize solution and the FA will take its initial position. And when *mnodes.dat* file will be read at the first iteration of the FSI coupled CFD simulation, no fluid movement will be induced by FA displacement.

Figure 1: Schematic presentation of FSI coupling algorithm in STAR-CCM+ simulation.

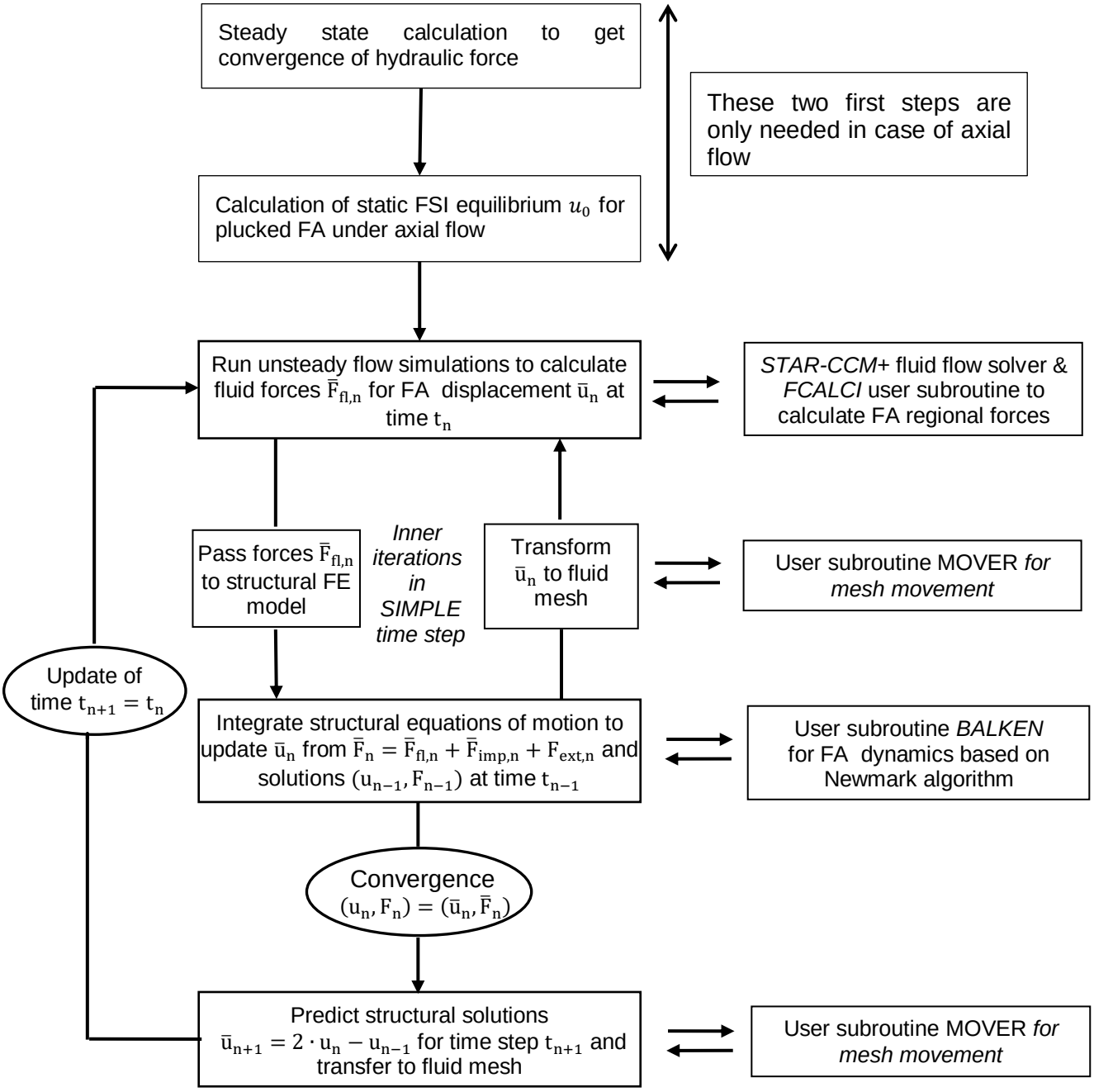

Figure 2: Scalar scene of the 15x0.5 FA after execution of *regsplit* subroutine.

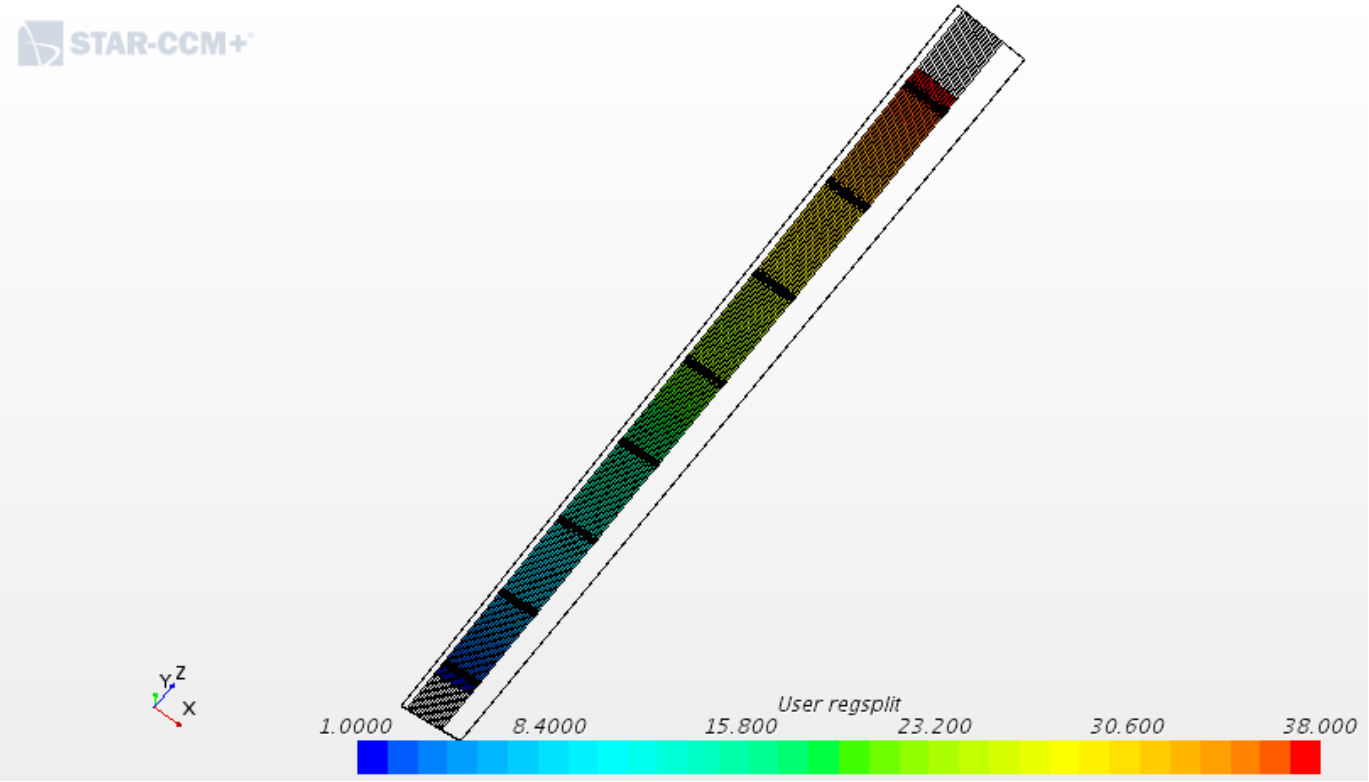

5. TEST FOR HTP 15x15 FUEL ASSEMBLY DESIGN IN STAGNANT WATER

5.1. CFD MODEL

The CFD geometry represents a sub channel HTP 15x0.5 with generic SG (cf. figure 3). The bottom and top nozzle are omitted. Instead we just add an extension of the fuel bundle.

The geometrical parameters are from the CAD model:

- STAR-CCM+ version: 11.04v010
- FR pitch / diameter: 14.4 mm / 10.92 mm
- SG height / width: 52 mm / 216.4 mm
- Basic cell size (24 cells per FR pitch) 0.6 mm
- Bypass (left/right) 30 mm / 113.6 mm
- Length of the FA 3913.5 mm

The full model (8 SG) involves ≈15 M fluid cells.

Each boundary of the fluid domain is considered as a wall except for lateral boundaries through the middle of the cross section witch are implemented as symmetry plane.

The values for density and dynamics viscosity are:

- $\rho = 992.3\ kg/m^3$, $\mu = 0.6531.10^{-3}\ Pa.s$.

These values came from the PETER loop test conditions ($T = 40\ °C$, $P = 1.5\ bar$)

The dynamic FSI couple CFD simulations are performed with

- Second order for the convection scheme.
- Second order for the time step integration scheme.
- SIMPLE algorithm with 30 outer inner iterations per time step.

For initial displacement from A_0 mm to 15 A_0 mm we have low Reynolds number

$$800 < Re = \frac{U.d_{FR}.\rho}{\mu} < 7000$$

and thus, no turbulence model is activated in CFD calculations. In order to calculate the Reynolds number, we estimate the maximum velocity value in the bundle flow area for the 1st eigenmode.

$$0.05\ m.s^{-1} < U \approx \omega.A.\frac{a}{a-1} < 0.42\ m.s^{-1}$$

ω, a and A are respectively the oscillation frequency, the maximum vibration amplitude and pitch to diameter ratio.

5.2. STRUCTURAL MODEL

For the damping matrix, $\alpha = 7.105\ 10^{-4}$ and $\beta = 0.7519$ which correspond to the first and eleven eigenfrenquency of a plug test in air.

The mass of the FA is M_{st} = 646.024 Kg. Moreover, the equation is

$$M_{st}.\underline{\ddot{u}} + D_{st}.\underline{\dot{u}} + K_{st}.\underline{u} = \underline{F_{fl}}$$

for this case. Time step of

$$\Delta t = 2.10^{-3}s$$

is sufficient to give good results according to sensitivity study.

Figure 3: Generic SG model for HTP 15x0.5 (FR in red).

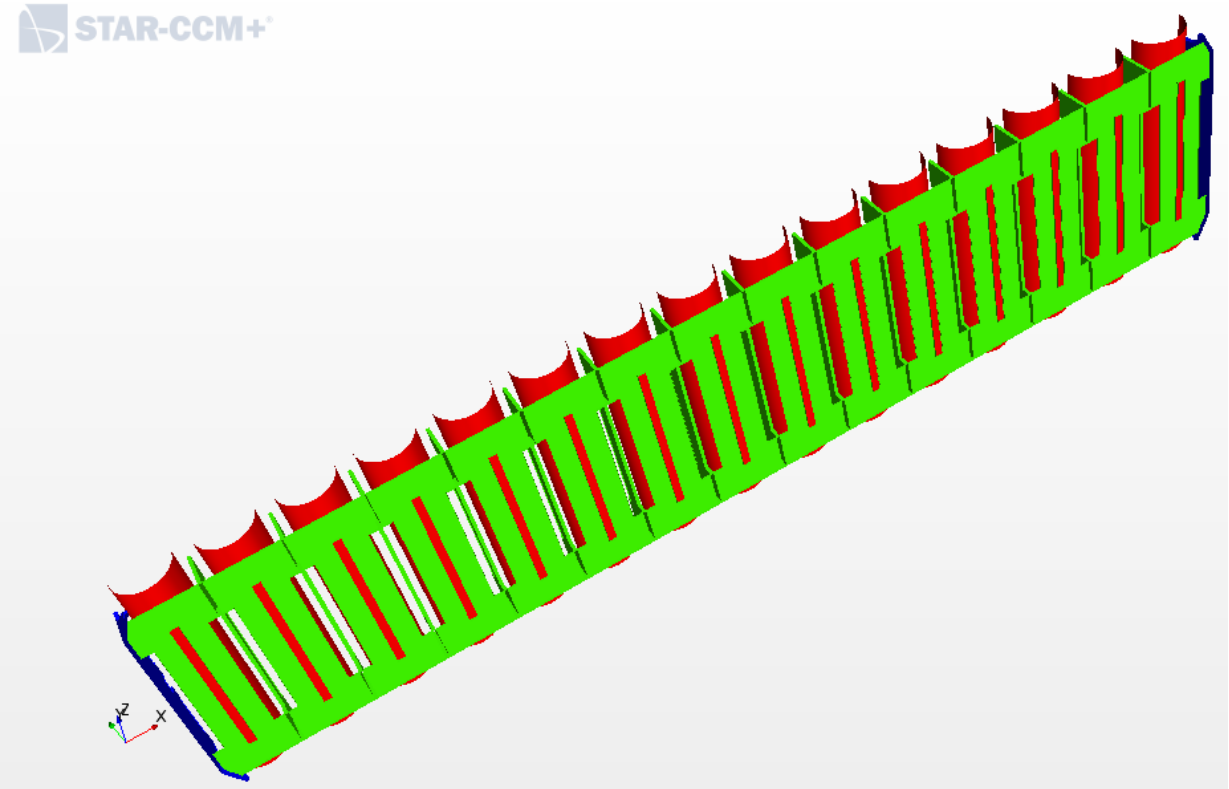

Figure 4: Mechanical beam model and CFD model from side view of 15x15 (FA region: red; Bypass region: blue; SG region= green)

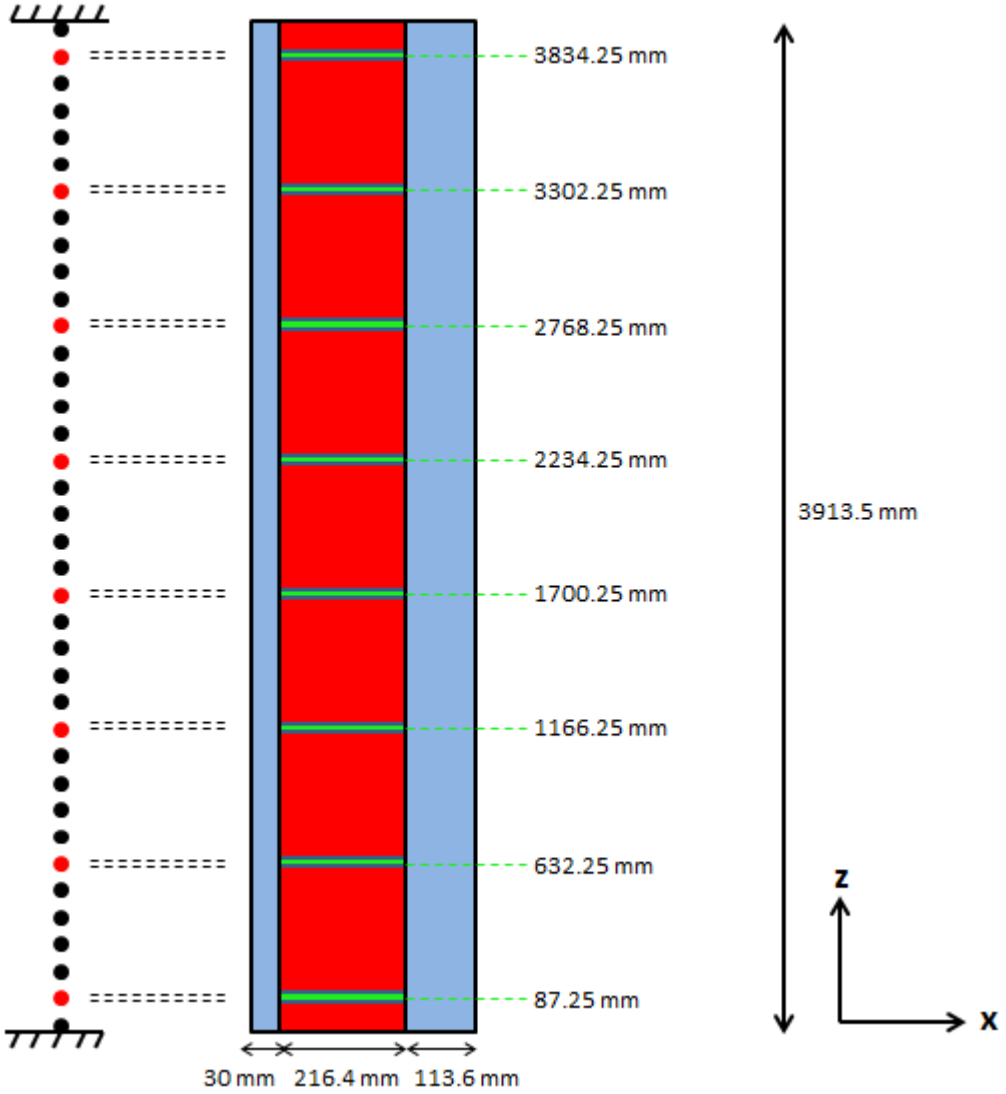

5.3. PLUG TEST AND SINUS SWEEP EXITATION RESULTS

For this model, five plug tests were realized with different initial amplitude (A_0 mm, 2.5 A_0 mm, 10 A_0 mm and 15 A_0 mm) and also three sinus-sweep tests with bottom and top excitation.

The idea is first to calculate the response of the FA for a plug test excitation with the “balken.f” Fortran program. The user coding implementation in the STARCCM+ software is benchmarked with the fluid solver frozen option. The results (cf. Figure 5) show a perfect concordance between the two simulation which mean that the coupling between STARCCM+ and the Usercoding is well implemented. Then we realize pluck tests excitation with taking into account fluid solver. We extract from these simulations data of structural displacement, respectively velocity and fluid forces.

From the values of the times at which the displacement achieves its maxima we can evaluate the damping ratio ζ and frequency f of the fundamental vibration mode with:

$$f = \frac{1}{T_{i+2} - T_i} \; ; \quad \frac{\zeta}{\sqrt{1-\zeta^2}} = \frac{1}{2\pi} \log \frac{A_i}{A_{i+2}} \tag{13}$$

As one can see Figure 6, A_i and T_i represent the amplitude maximum and its corresponding time.

Figure 5: Comparison of a 5 A_0 mm pluck test in air at SG5 between BALKEN Fortran code and FSI implementation in STAR-CCM+ (fluid solver frozen).

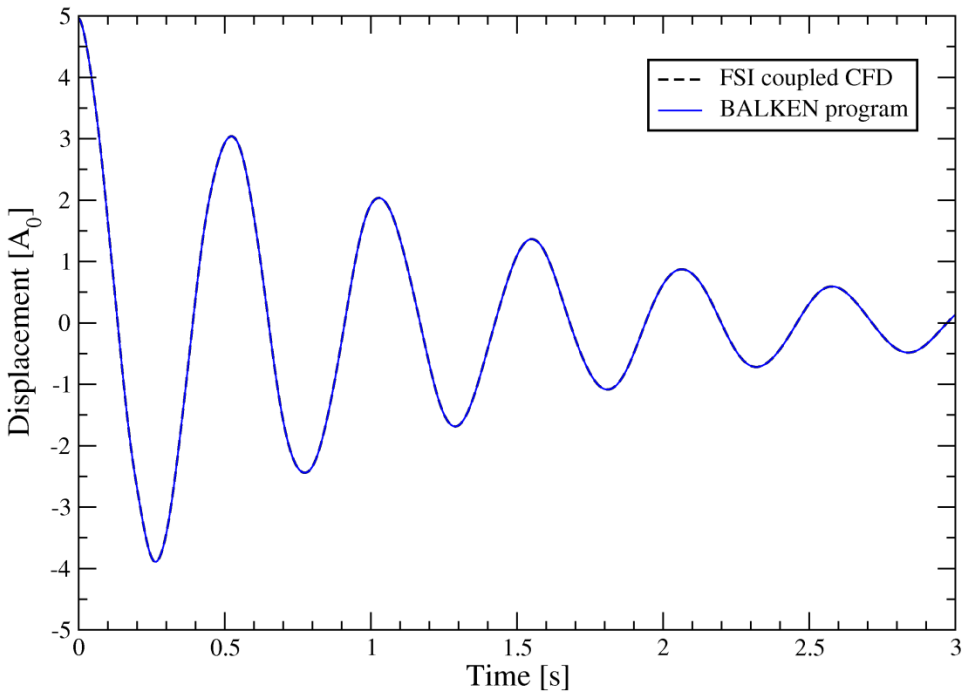

To understand the origin of these formula, one needs to recall that the solution of equation of motion is

$$u(t) = A.e^{-\zeta.\omega_n.t}\cos(\omega_d.t - \phi) \tag{14}$$

with

$$\omega_d = \sqrt{1-\zeta^2}.\omega_n \tag{15}$$

where ω_n is the natural circular frequency and ω_d denote the damped circular frequency. With a decrement logarithm we get

$$\Delta = \ln u_1 - \ln u_2 = \ln \frac{u_1}{u_2} \tag{16}$$

Now we combine Eq. (14) and Eq. (16) and consider a 2π period

$$\frac{u_1}{u_2} = e^{\zeta.\omega_n.(t_2 - t_1)} \tag{17}$$

Figure 6: Damping characteristic in air and stagnant water at SG 5 for a 15 A_0 mm pluck test using FSI coupled CFD simulations.

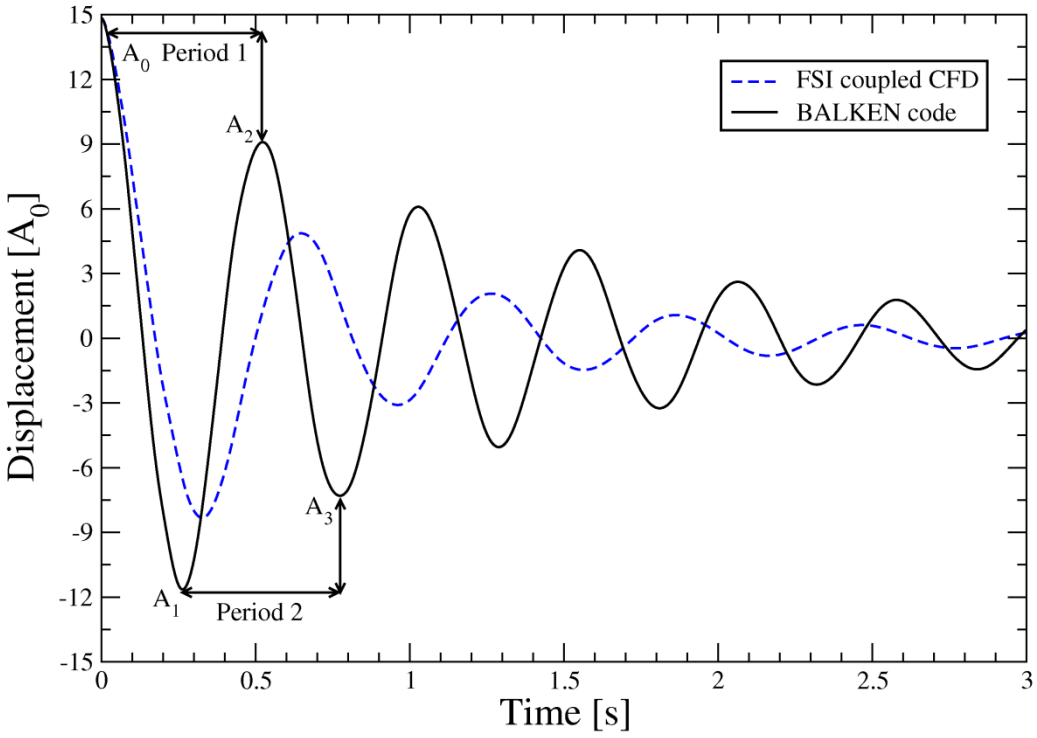

We know that

$$f = \frac{1}{t_2 - t_1} \leftrightarrow \omega_d = \frac{2\pi}{t_2 - t_1} \tag{18}$$

and then we finally get

$$\ln\frac{u_1}{u_2} = \zeta.\omega_n.(t_2 - t_1) = \zeta.\omega_n.\frac{2\pi}{\omega_d} = \frac{\zeta.2\pi}{\sqrt{1-\zeta^2}} \tag{19}$$

By reordering Eq. (19) we confirm Eq. (13) We now use the software package Mathematica to extract maximum and minimum and to solve Eq. (13)

The first oscillation is not used for the damping evaluation since we consider it is not a free oscillation. This is because of the impact $(t = 0s)$ on the FA and transient phenomena. Then we use the other values of free oscillation starting with period 2 $(A_1 \rightarrow A_3)$ to extract damping values. One can also see in Figure 6 the damping impact on the amplitude and frequency.

One needs to know that a pluck test simulation takes twelve hours to compute on 224 cores. It will be interesting to do the calculation with the BALKEN Fortran code which takes less than one second. In order to realize this, we need to have an idea of the fluid mass and damping matrix. The latter are linked to the fluid force by the relation:

$$\underline{F_{fl}} = -M_{fl}.\underline{\ddot{u}} - D_{fl}.\underline{\dot{u}} - K_{fl}.\underline{u} \tag{20}$$

We can neglect the contribution of $K_{fl}.\underline{u}$ term, since we don´t have any axial flow. And it exist a non-linear relation between the damping and the velocity:

$$D_{fl} = \delta\,.|\dot{u}| \tag{21}$$

where δ is the water damping constant.

From the STARCCM+ simulation we extract the fluid forces on the beam nodes and use them to approximate the nodal fluid masses and the water damping constants with a least square procedure. In this approach, we assume the fluid matrices to be diagonal, i.e., neglect fluid coupling effects between the beam nodes. Then if we combine Eq. (1) and Eq. (20) and rearrange, we obtain:

$$\left(M_{st} + M_{fl}\right).\underline{\ddot{u}} + \left(D_{st} + D_{fl}\right).\underline{\dot{u}} + K_{st}.\underline{u} = 0 \qquad (21)$$

By solving this equation with the BALKEN Fortran code we should get the same results of a pluck test in stagnant water with STARCCM+.

The results are in a good agreement for small initial amplitudes (cf. Figure 7). After the two first oscillations there is a slight difference between the two curves. This is due to damping mechanisms in the CFD FSI simulations that are not captured by the simplified FSI description in the BALKEN code and also because the least square procedure induced approximation.

Figure 7: Comparison of the displacement time histories at SG 5 for A_0 mm, 2.5 A_0 mm, 10 A_0 mm and 15 A_0 mm between dynamic CFD coupled FSI simulation (STARCCM+) and the BALKEN Fortran code.

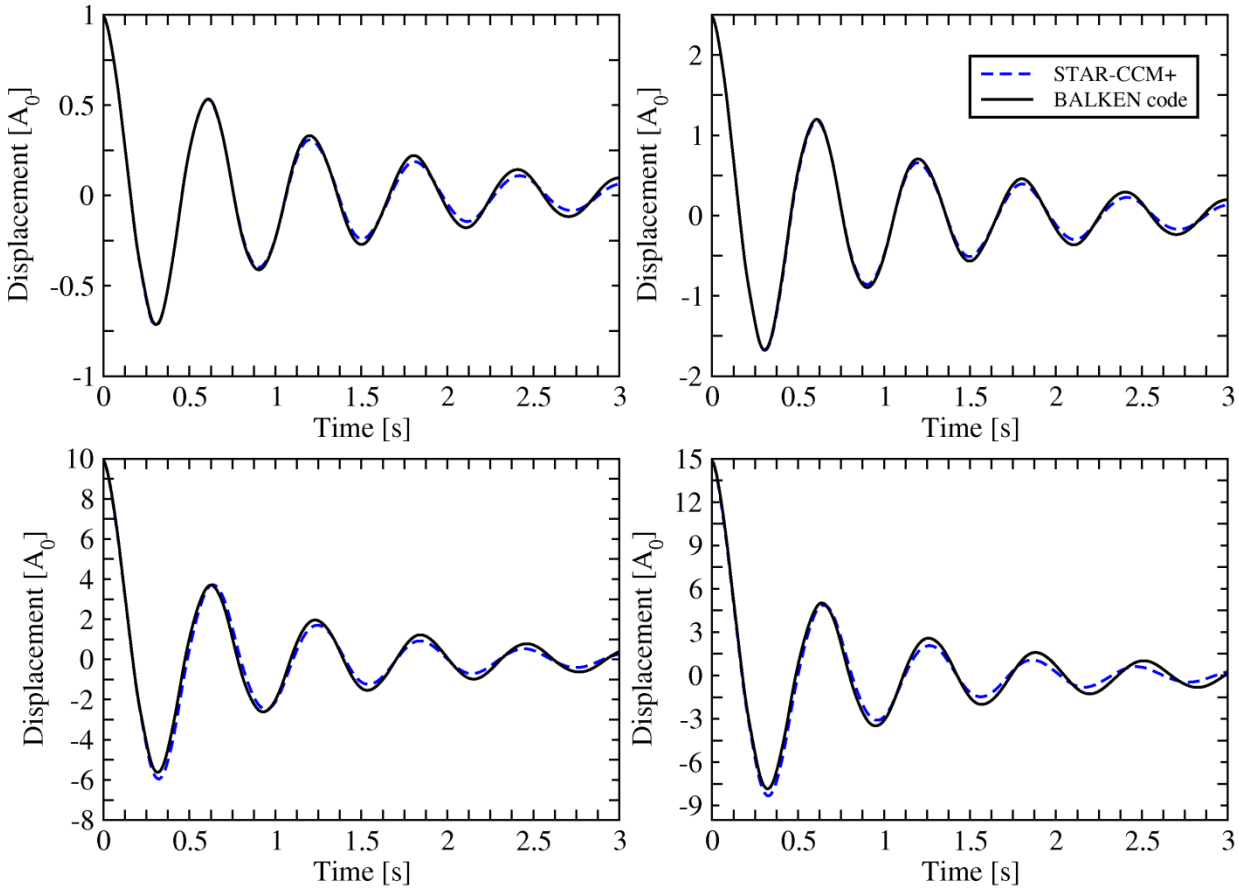

With the calculated hydraulic forces from the CFD solver as input, the BALKEN code reproduces the damping characteristic of the FSI coupled CFD simulations (see Figure 8). The still visible small deviations originate from the employed under relaxation procedure in the displacement solution between the inner FSI iterations of a time step in the FSI coupled CFD simulations.

From Table 1, we calculate a fluid mass average of 412.22 Kg. This value should be constant, but error is below 5% for all values which is acceptable for our case. Concerning damping values, we should get consistent values between the different pluck test which appears to not be the case. This is probably

due to boundary effects. Though without the first five nodes we can still observe some difference between damping values.

Table 1: Added fluid mass and damping over the full FA derived from the linear square procedure for pluck test.

Initial displacement [mm]	Added fluid mass [kg]	Fluid damping [m^2/s] Nodes 2 to 39 - 7 to 34	Structural mass [Kg]
A_0	417.393	45813.9 - 76.486	641.217
2.5 A_0	403.475	19726.7 - 37.891	
5 A_0	401.015	113451.1 - 28.147	
10A_0	413.787	6995.6 - 23.151	
15A_0	425.442	5471.9 - 21.277	

Figure 8: Comparison of displacement time histories at SG5 for A_0 mm, 2.5 A_0 mm, 10 A_0 mm and 15 A_0 mm between STARCCM+ and the BALKEN Fortran code (hydraulic forces from STAR-CCM+ as entry).

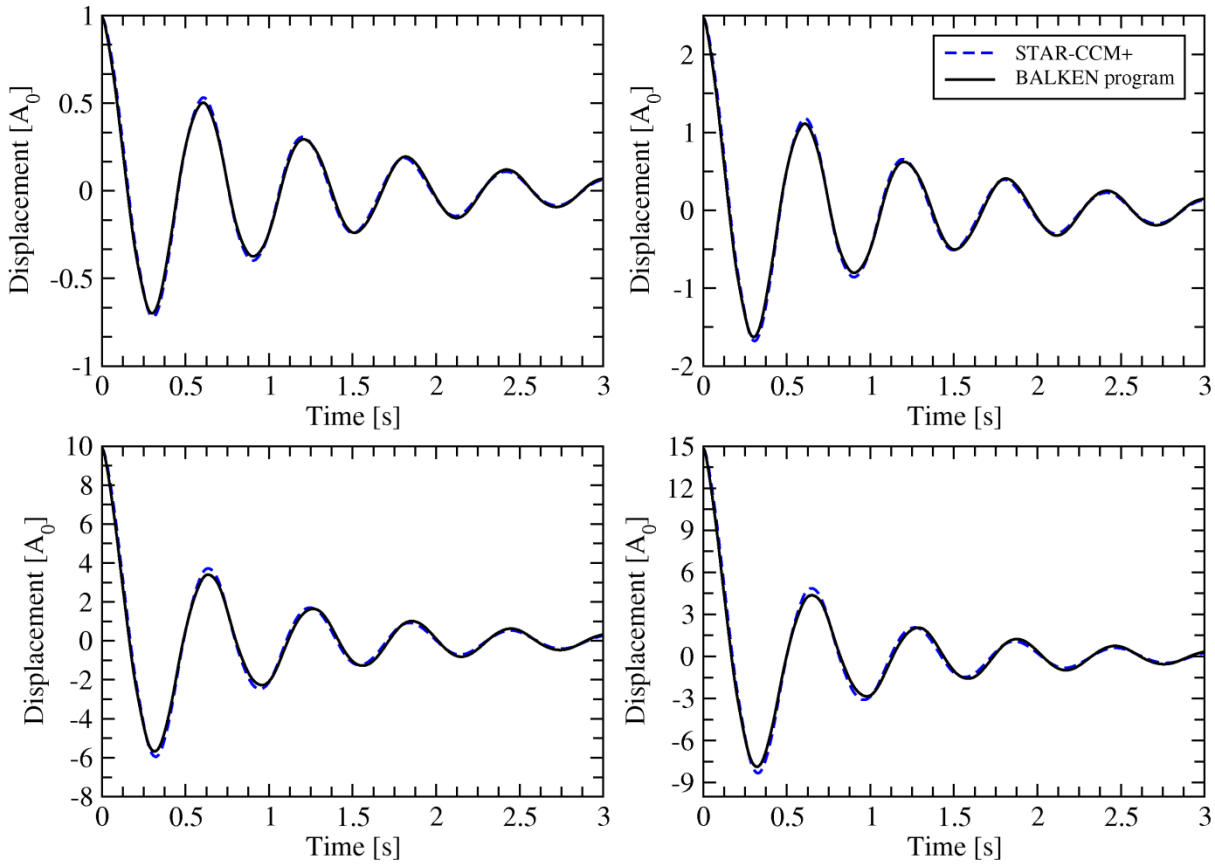

We now want to collect damping values from sinus sweep tests. The latter employed a different methodology since we applied an acceleration excitation of the water reservoir containing the FA:

$$\ddot{X}_0(t) = A_0 \sin(2\pi \frac{f_1}{Rlog(2)} (\exp(\log(2)\, RT) - 1) \tag{22}$$

A_0 = 150/300/600 mm/s^2, f_i = 1 Hz and R = 1/20 s^{-1} are respectively the maximum vibration amplitude (constant), start frequency and sweep rate (constant). The displacement response of the FA is calculated with the equation of motion Eq. (1) where we add structural inertial forces for this case

$$F_{ext}(t) = -M_{st}.\underline{\ddot{X}_0} \tag{23}$$

with $\underline{\ddot{X}_0}$ is the acceleration of the water container. In this case, if the user is outside the moving system the equation of motion is written as:

$$M_{st}.\ddot{X} + D_{st}.\dot{X} + K_{st}.X = -M_A.\ddot{X} - M_c.\ddot{X}_0 - \delta|\dot{X} - \dot{X}_0|.(\dot{X} - \dot{X}_0) \tag{24}$$

where $\underline{\ddot{X}} = \underline{\ddot{X}_0} + \underline{\ddot{x}}$ is the total acceleration and $\underline{\ddot{x}}$ the FA acceleration. M_A denote the added mass matrix and M_C is the coupled mass matrix. This equation can be rearranged to

$$M_{st}.(\ddot{X}_0 + \ddot{x}) + D_{st}.\dot{X} + K_{st}.X = -M_A.\ddot{x} - (M_A + M_C).\ddot{X}_0 - \delta.|\dot{x}|.\dot{x} \tag{25}$$

If we consider that we are looking at the deformation from inside the system, we have:

$$(M_A + M_{st}).\ddot{x} + D_{st}.\dot{x} + K_{st}.x = -(M_{st} - M_D).\ddot{X}_0 - \delta.|\dot{x}|.\dot{x} \tag{26}$$

Therefore, we can obtain a relation between the coupled mass, the edit mass and the displaced mass M_D.

$$M_A + M_C = -M_D \tag{27}$$

This equation is needed to pass from one to another system representation. In seism study, one will always work with the total acceleration thus with the coupled mass matrix. In our case we place ourselves inside the system and therefore talk about displaced mass. The goal is now to approximate these two matrices and one remake the same method as previously used with pluck test. We use a least square regression to extract the added mass, displaced mass matrix and the damping constant of the fluid force

$$F_{fl} = -M_A.\ddot{x} + M_D.\ddot{X}_0 - \delta.|\dot{x}|.\dot{x} \tag{28}$$

The values from pluck tests and sinus sweep excitation are reported in Table 3. In order to avoid any boundary effect, we took values from beam nodes 6 to 35.

Table 2: Extracted values from least square method.

	A_0 mm	2.5 A_0 mm	4 A_0mm	5 A_0mm	10 A_0mm	15 A_0mm	150 mm/s^2	300 mm/s^2	600 mm/s^2
M_A	202.54	190.953	191.035	193.242	209.795	222.113	200.96	208.36	219.483
M_D	-	-	-	-	-	-	87.974	75.119	69.340
δ/D_0	1406.6	681.8	535.67	485.99	385.99	349.16	583.96	464.67	404.47

One can see a good agreement between the results. Higher amplitude, such as pluck test 30 mm and sinus sweep 600 mm/s^2, leads to slightly higher values of added mass. It might be that a higher order expansion of the fluid damping forces would help to reduce the differences.

From the least square method we also have extract values of displaced mass for the three sinus sweep excitation. One way to confirm that we have accurate results it´s to check consistency between the latter displaced mass and the geometrical value we can extract from STAR-CCM+ as follow: we first calculate the fluid volume with a report for threshold part (z=0; z=3913.5 mm), $V_{fluid} = 7.39704.10^{-3}$ m^3. Then we use the total volume $\frac{14.4}{2} mm * (216.4 + 113.6 + 30) mm * 3913.5\, mm = 10.143792\ 10^{-3}$ m^3. By using M=ρ*V ($992.3 * (10.143792\ 10^{-3} - 7.39704.10^{-3}) * 30$), we find 81.77 Kg for the displace mass. The factor 30 is needed since the model has been reduce to 15x0.5. One can easily notice the consistence between the three displace mass from the sinus-sweep tests and the

one calculated from STAR-CCM+. In Figure 9, one can see the impact of the water damping on the displacement response of the FA.

By using the half-power method, we can approximate damping ratio with:

$$\zeta = \frac{f_2 - f_1}{2.f_0} \tag{29}$$

Where the frequency f_1 and f_2 correspond to $\frac{1}{\sqrt{2}}$ of the maximum peak f_0. That is shown in Figure 10 which is for sinus-sweep test at excitation amplitudes $A_0 = 300\ m.s^{-2}$. Basically, the transfer function

$$|X(f)| = \frac{1}{\sqrt{[1 - \left(\frac{f}{f_n}\right)^2]^2 + [2.\zeta.\left(\frac{f}{f_n}\right)]^2}} \tag{30}$$

Figure 9: Displacement response of the FA at SG 5 in air and water for A_0=300 mm/s^2.

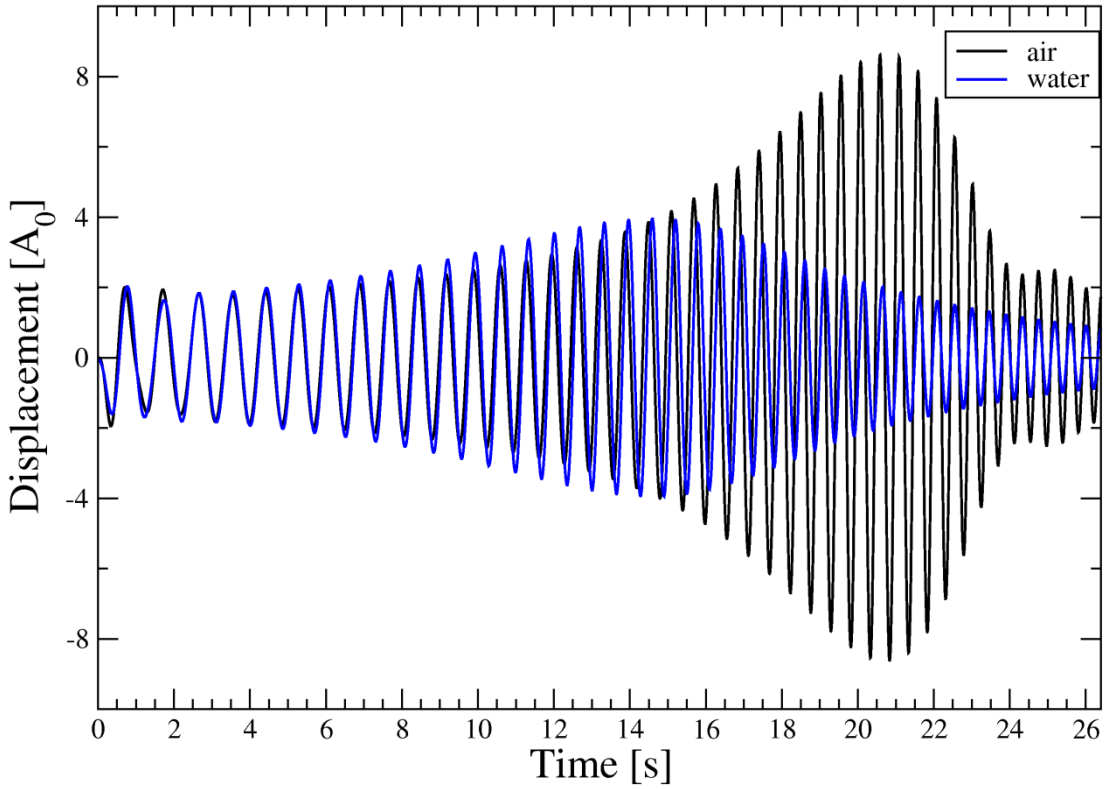

has its maximum value equal to

$$|X_{max}(f_0)| = \frac{1}{2.\zeta}.\sqrt{1 - \zeta^2} \tag{31}$$

If one consider small values of damping the following approximation can be made:

$$|X_{max}(f_0)| \cong \frac{1}{2.\zeta} \tag{32}$$

To calculate ζ we consider two frequency points f_1 and f_2 with the assumption that $f_2 > f_1$ on either side of $X_{max}(f)$:

$$|X(f_1)| = |X(f_2)| = \frac{1}{\sqrt{2}}.|X_{\max}(f_0)| \tag{33}$$

Combining Eq. (30) and Eq. (32) we obtain

$$(f/f_0)^2 - 2.(1-2.\zeta^2).\left(f/f_0\right)^2 + (1-8.\zeta^2) = 0 \tag{34}$$

Solution of Eq. (34) for the case of two real roots leads to

$$(f/f_0)^2 = (1-2.\zeta^2) \pm 2.\zeta.\sqrt{1+\zeta^2} \tag{35}$$

Figure 10: Displacement at SG5 function plot with an excitation amplitude $A_0 = 300\ mm.s^{-2}$ (16.8 % of structural + fluid damping).

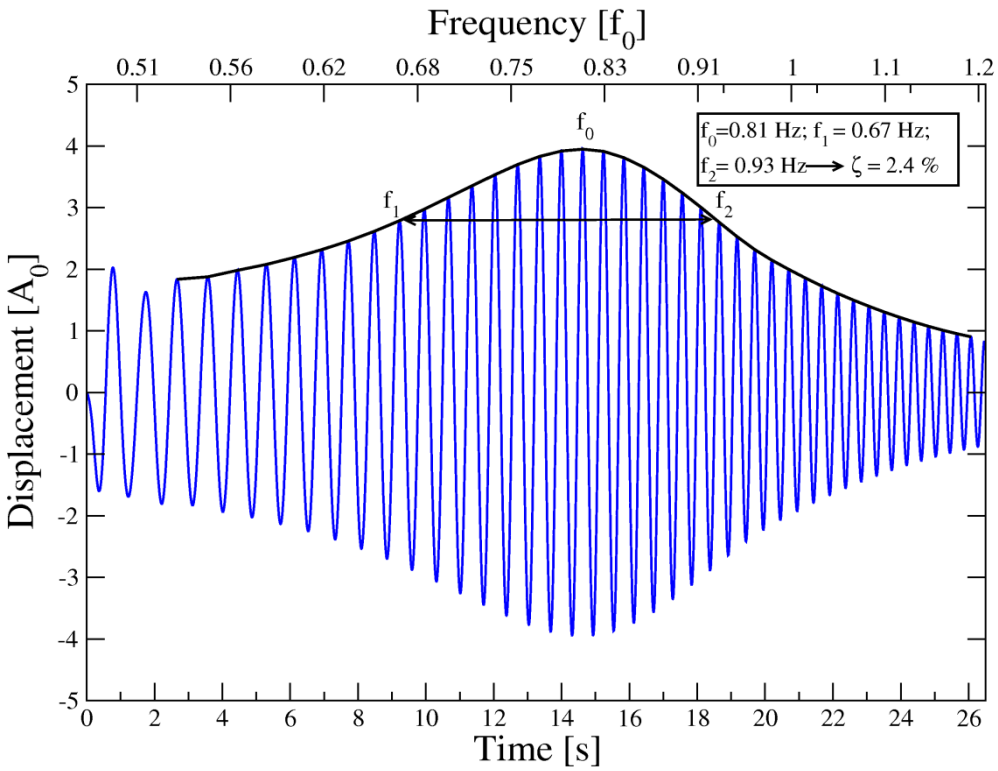

The final step is to expand this expression in a Taylor series and we finally get

$$2.f_0.\zeta = f_2 - f_1 \tag{36}$$

One has to take into account that approximations has been made to get this result and that Eq. (29) is useful only with small damping ratio (ζ<0.383 according to [2]).

Table 3 summarize the results from the three sinus sweep excitation tests. Damping values are under 30% hence as discuss we should have accurate values. Further simulations with higher initial amplitude are not needed as far as damping values will be higher than 38.3% and then not useful with our extracting damping method.

Table 3: Damping ratio of the sinus sweep excitations of the FA at SG5.

Amplitude A_0 $[mm.s^{-2}]$	f_1-f_2 [Hz]	f_0 [Hz]	ζ [%]
150	0.707 – 0.936	0.83	1.12
300	0.673 – 0.926	0.81	1.31
600	0.385 – 0.678	0.78	1.72

Figure 11: Comparison of the displacement time history at SG level 5 produce by sinus sweep excitation (A_0=300 mm/s^2) between CFD coupled FSI simulation and Balken Fortran code.

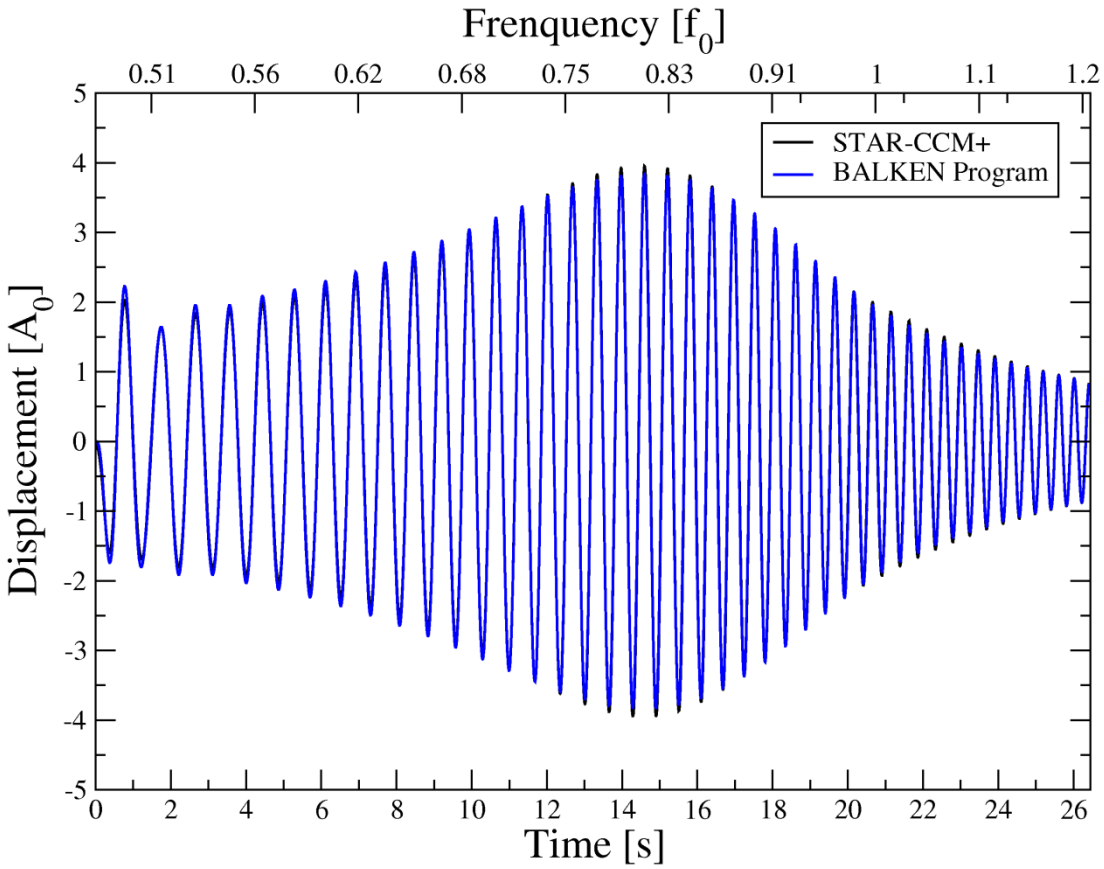

One can see in Figure 11 that the sinus-sweep test calculation with the Balken code featuring fluid mass and damping terms leads to a very good agreement with FSI coupled CFD simulation. Therefore, the fluid force expansion according to Eq. (28) is more suitable for sinus sweep excitation than for pluck test. Since an FSI coupled sinus-sweep test simulation with CFD takes approximately three days to compute on 240 cores it becomes profitable to use the FSI implementation in the Balken Fortran code.

Figure 12: Water damping of a 15 A_0 mm pluck test at SG level 5 including 3 sinus sweep excitation (150/300/600mm/s^2).

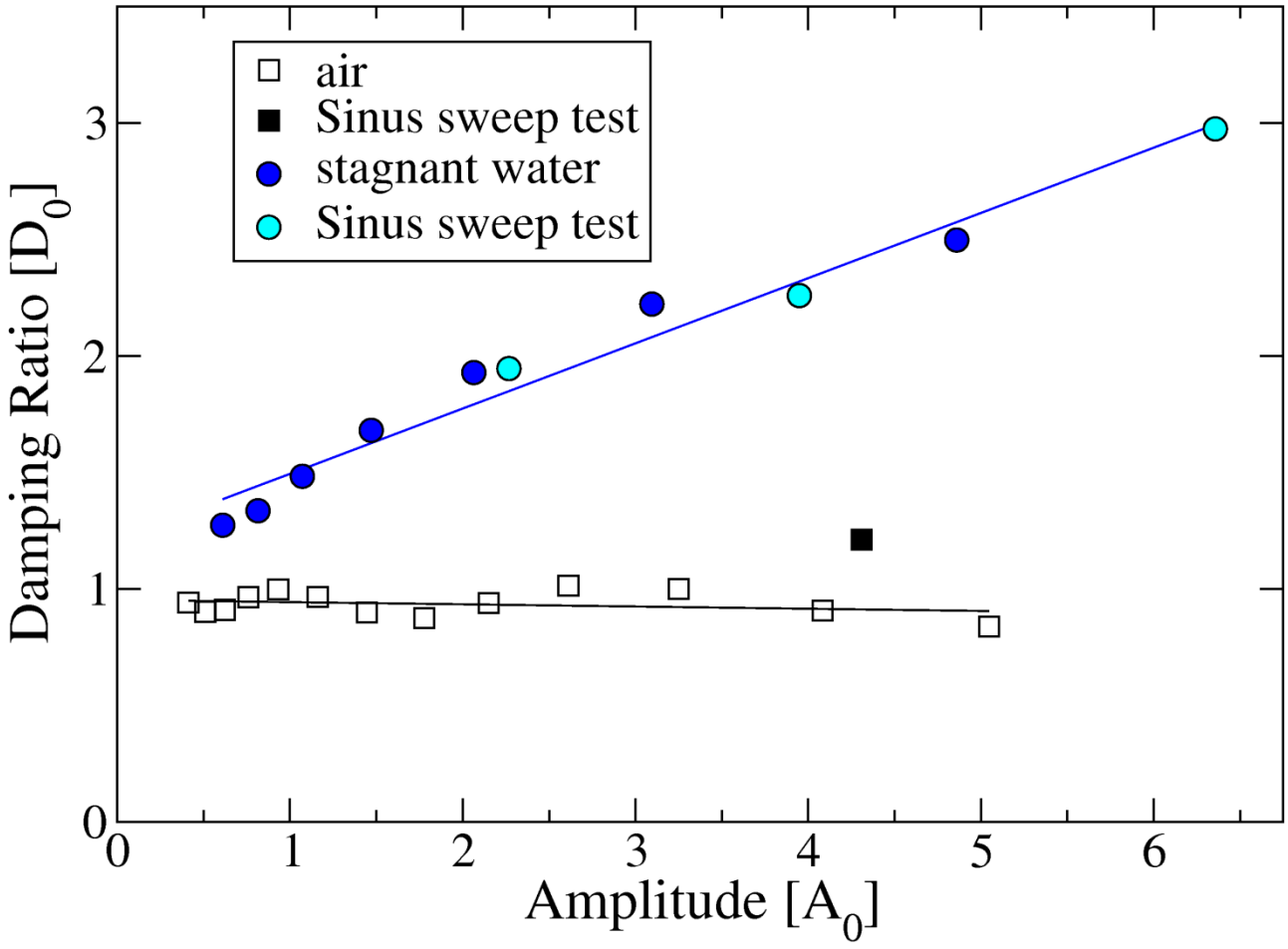

Figure 12 presents the results of the 15 A_0 mm pluck test and three sinus sweep excitation with 150, 300 and 600 mm/s^2 max vibration amplitude. We choose to represent pluck test with 15 A_0 mm initial because of its larger range of damping points. One can easily observe the good agreement between the results. The fact that the trend line doesn't fit perfectly for all points it´s mainly because of non-linear fluid effects that are not in line with the simple approximation of the fluid damping force according to Eq. (28).

One can see that values from sinus sweep test are slightly shifted compare to pluck test values in Figure13. The difference between the values can be explained by the fact that the two excitation mechanisms are different and hence give slightly different results (deviation ≈ 5%). But one can notice that the gap between the point of sinus sweep excitation in air and trend line of pluck test in air is approximately the same as the one between point of sinus sweep in water and the trend line of the pluck test in water. Moreover, one can easily notice the trend is to decreasing frequency with increasing amplitude and the trend is to increasing damping with increasing amplitude values. The frequency lowering in water is due to the added fluid mass and amounts to ≳ 20% in good agreement with SHP-1 test measurement results for other fuel designs.

Figure 13: Frequency in function of amplitude at SG level 5 for 15 A_0 mm pluck test and three sinus sweep excitation (150/300/600mm/s^2).

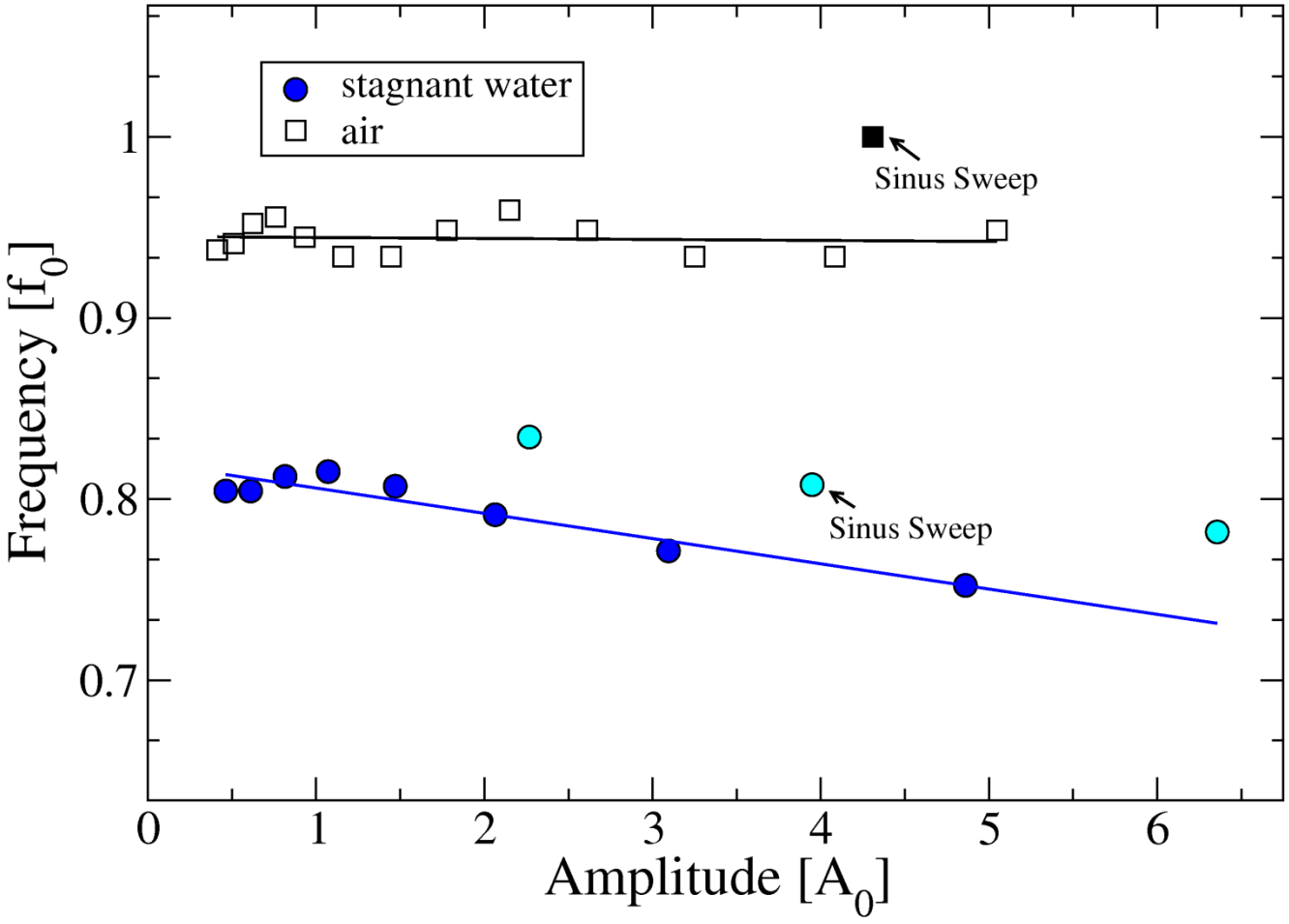

From FSI coupled CFD simulation we can also extract physical values for each beam nodes. This is one of greatest advantage of these simulation compare to experience in which it is not possible to have access to such values. Table 4 presents the distribution of the added, displace and structural mass at beam nodes location. In this case, we consider that there is one beam node at each spacer grid level and one beam node in-between two spacer grids (French approach). Regarding water damping values at beam nodes 2 and 14 we observe that we have strong boundary effect.

Thanks to sinus sweep excitation and pluck test we were able to extract damping and mass values. The goal there was not to benchmark our results with experimental test but more to take in hand STAR-CCM+ and the BALKEN Fortran code. We also tried to optimize the work flow by reproducing FSI coupled CFD simulation with the BAKLEN code. The results from this evaluation are in good agreement and can be used if simulation need to be run in the near future. Besides, we did some constant check to have an idea if our results were in good agreement with reality or not. In order to confirm that our model is valid, a sensitivity study is made in Section 4.4. In the next Section we study the existence of confinement effect.

Table 4: Damping constant, added, displace and structural mass values for each beam nodes for FSI coupled CFD sinus-sweep simulation (150mm/s^2).

Beam nodes	Added mass [Kg]	Damping constant	Displace mass [Kg]	Structural mass [Kg]
2	29.592	559.76	6.975	52.185
3	19.884	81.44	6.333	48.130
4	15.770	39.55	6.027	44.075
5	16.638	37.43	6.283	44.075
6	15.286	29.57	6.223	44.075
7	16.902	32.63	6,178	44,075
8	15.524	27.87	6.018	44.075
9	16.873	37.81	6.279	44,075
10	15.289	29.90	6.227	44.075
11	16.627	37.81	6.279	44.075
12	15.885	40.81	6.007	44.075
13	19.873	84.69	6.281	47.263
14	29.360	616.5	6.674	50.451
Summation	243.504	1655.8	81.693	594.706

5.4. CONFINEMENT EFFECT

Confinement effect could easily appear when the space between the FA and another FA (wall in our case) is really small. The eigenfrequency could be affected by this kind of effect. Therefore, we need to have an idea of their prominence. In order to capture these confinement effects, we now consider a symmetric bypass. We choose to test it for the following configuration:

- 12 mm bypass / 10 mm initial amplitude;
- 10 mm bypass / 8 mm initial amplitude;
- Sinus sweep excitation 2.5 mm bypass / 50 mm/s^2

The three tests will be compared to simulation with the original asymmetric design (i.e 30mm-113.6mm bypass) in which we consider that the bypass is wide enough to notice confinement effect.

As one can observe in Figure 14 and Figure 15, no noticeable confinement effect exists. Even if there is a slightly shift between the two curves ($\leq 1\%$) for both 6 A_0 mm bypass and 5 A_0 mm, it can be considered as negligible.

Figure 14: Comparison of pluck test with 5 A_0 mm initial amplitude at SG5 between symmetric 12 mm bypass and asymmetric 30 mm – 113.6 mm.

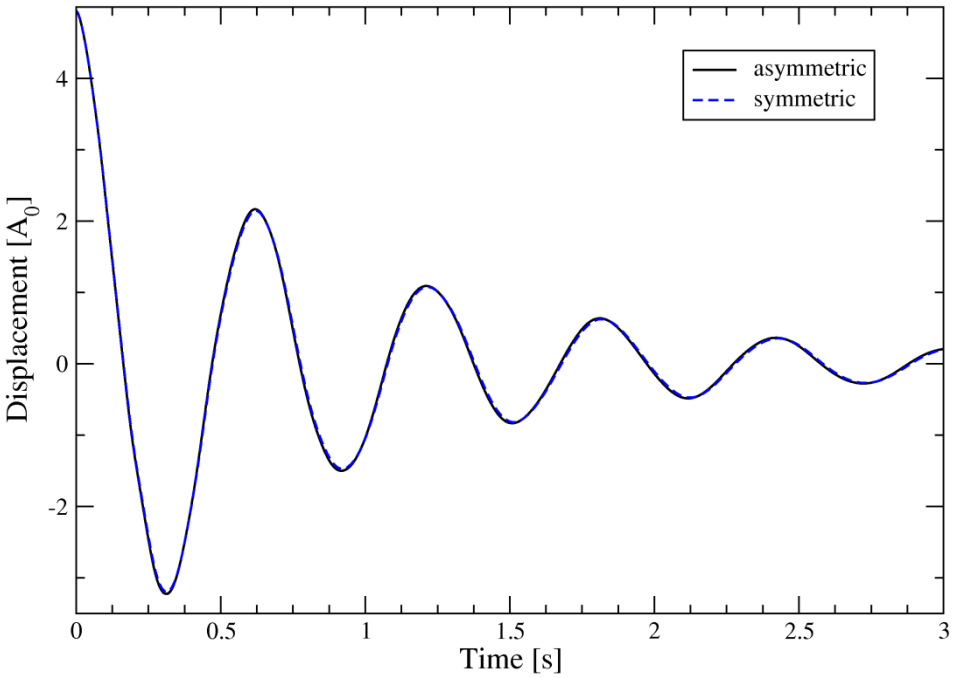

Figure 15: Comparison of pluck test with 4 A_0 mm initial amplitude at SG5 between symmetric 10 mm bypass and asymmetric 30 mm – 113.6 mm

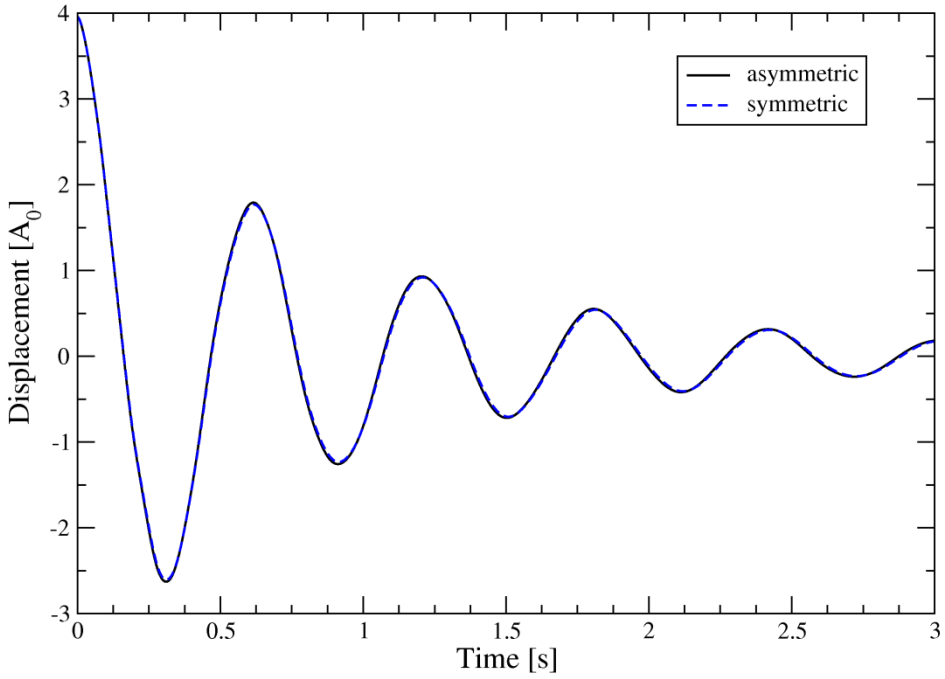

5.5. SENSITIVITY STUDY

By doing a sensitivity study we assure in a way the robustness of the results. For this study we took as variable:

- Number of inner iterations [30 to 40];
- Times step [2.10^{-3} s to 1.10^{-3} s];
- Convergence tolerance for the resolution of velocity and pressure solver [0.1 to 0.01];

These FSI coupled CFD simulation will be compute for a 10 A_0 mm pluck test and benchmark with the setting of the initial design (see section 4.1).

Figure 16: Comparison of pluck test with 5 A_0mm initial amplitude at SG5 for different input parameters (Reference curve: 30 inner iteration; 0.002 time step; 0.1 convergence tolerance).

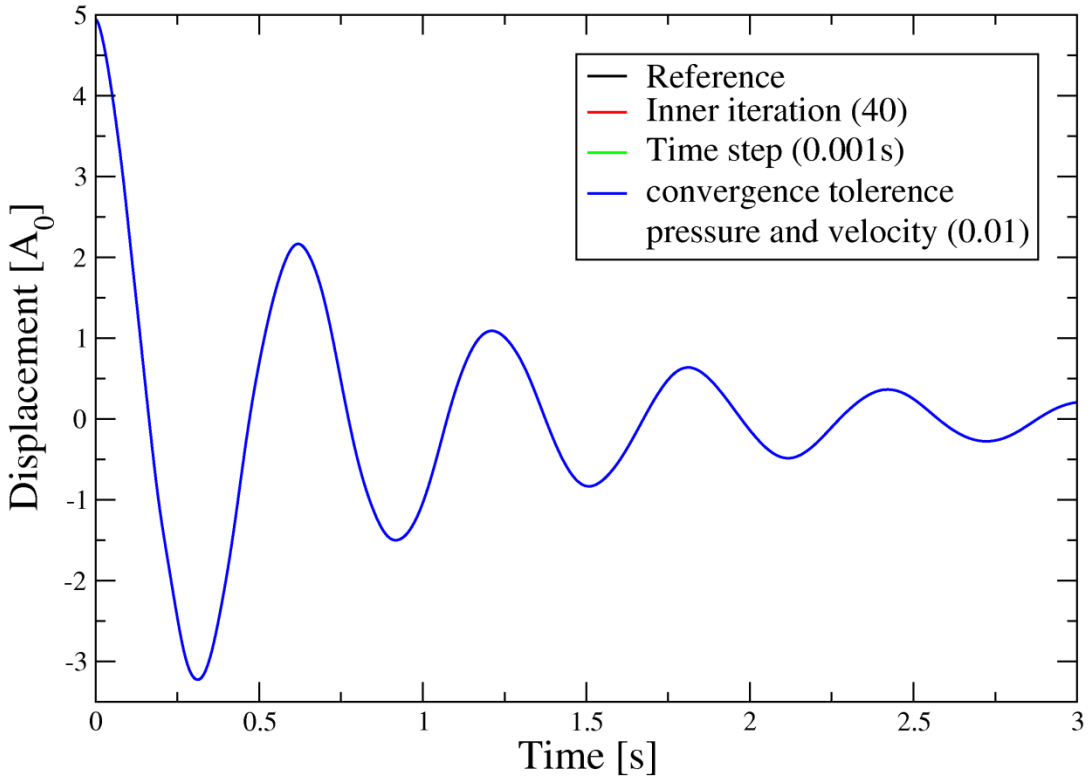

In Figure 16, one can observe that the curves are in a perfect agreement with the different input parameters such as the number of iterations, the time step and the convergence tolerance. In order to get some information and to validate our model, we have therefore simulated pluck test with finer inputs. For further deepening of this HTP 15x0.5 model one can try to run simulation with finer mesh and also with γ = 0.1. Moreover, it could be worthwhile to run simulation with a coarser mesh (i.e. 0.8 mm basic cells). Indeed, if one finds a good agreement with the previous results and since the size of the model will be smaller we could save numerical cost.

6. TEST FOR HTP 8x8 SCALED DESIGN UNDER AXIAL FLOW

6.1 CFD MODEL

The CFD geometry represents an HTP 8x4 with 10 detailed SG (From CAD geometry, cf. Figure 18). The bottom and top nozzle are omitted. Instead we just add an extension of the fuel bundle. These simplifications are made to save some numerical cost.

The geometrical parameters are from the CAD model:

- STAR-CCM+ version 13.02v011
- FR pitch / diameter: 12.6 mm / 9.5 mm
- GT diameter: 12.45 mm
- SG height / width: 44.45 mm / 100.6 mm
- Basic cell size (24 cells per FR pitch) 0.3145 mm
- Bypass (left/right) 30 mm / 113.6 mm
- Length of the FA 4550.5 mm
- Boundary layer thickness on FR / SG surface: 0.15mm / 0.1 mm

The full model (10 SG) involves ≈ 200 M fluid cells. To determine this setting a sensitivity study has been realized which provide a wall distance $y^+ = 30$ for the employed RANS turbulence models [3].

The inlet of the FA is set as velocity inlet with 5 m/s, 0.05 for turbulence intensity and 1mm for characteristic length. Outlet is set as free outlet. FSI and walls are set as wall type. And the lateral boundary where the FA has been cut in a half is set as symmetry plane (cf. Figure 17).

FSI structural code is applied on the FA from z = 0 to z = L (cf. Figure 19).

The values for density and dynamics viscosity are:

- $\rho = 992.3\ kg/m^3$, $\mu = 0.6531.10^{-3}\ Pa.s$.

These values came from the PETER loop test conditions ($T = 40\ °C$, $P = 1.5\ bar$).

Figure 17: Cross section of the CFD model with indications of the dimensions for FA and bypass geometry (FR: green; bypass: blue; SG: red).

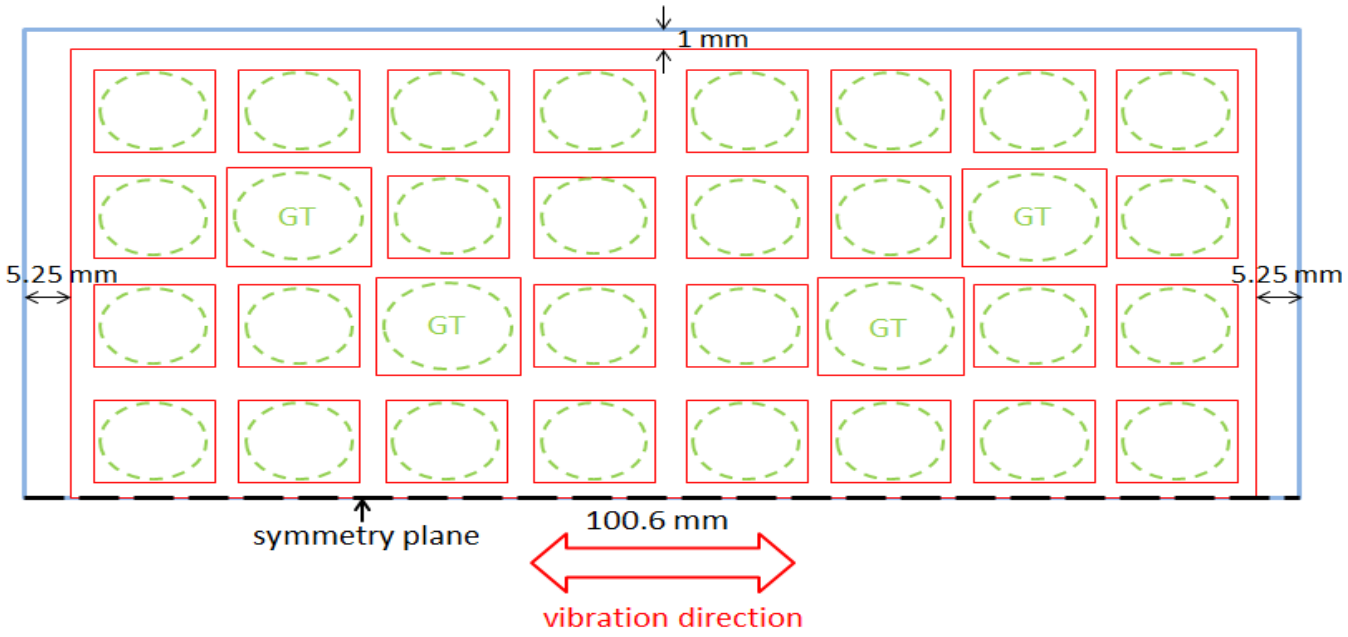

The Reynolds number

$$Re \approx 100000$$

underlines our choice to set turbulence model on. As shown in Figure 1, the first step is to calculate static FSI equilibrium of the FA which is done with the following setting:

- 1st order time integration scheme.
- SIMPLE algorithm with 10 inner iteration

For dynamic FSI coupled CFD simulations:

- 2nd order time integration scheme.
- SIMPLE algorithm with 20 inner iteration

For the damping matrix, $\alpha = 7.864\,10^{-4}$ and $\beta = 0.833$, which correspond to the first and eleventheigenfrequency in air.

In order to get a good and faster convergence of quasi steady simulations we first run a steady simulation with the standard k-eps model. The latter is taken as starting point for the quasi steady simulations. Quasi steady state simulations are needed since the fuel bundle are under axial flow and thus the water flow induced some bow response. Besides, this is exactly what is happening in the test at PETER loop. When the static FSI equilibrium is reach (after 1000 time steps $\Delta x < 10^{-3}$ mm) we took the new shape of the FA and impose them as initial shape for the pluck tests (unsteady simulation). We run each unsteady simulation for 0.8s physical time for the reason that amplitudes are incredibly low (high damping) after this value according to test results. Pluck tests are realized with 2.8 mm as initial amplitude. We have run pluck tests with several turbulence model (Standard k-eps, Standard k-eps quadratic, Realizable k-eps, k-omega SST, V2F).

Figure 18: HTP 8x4 space grid geometry in the detailed CFD model.

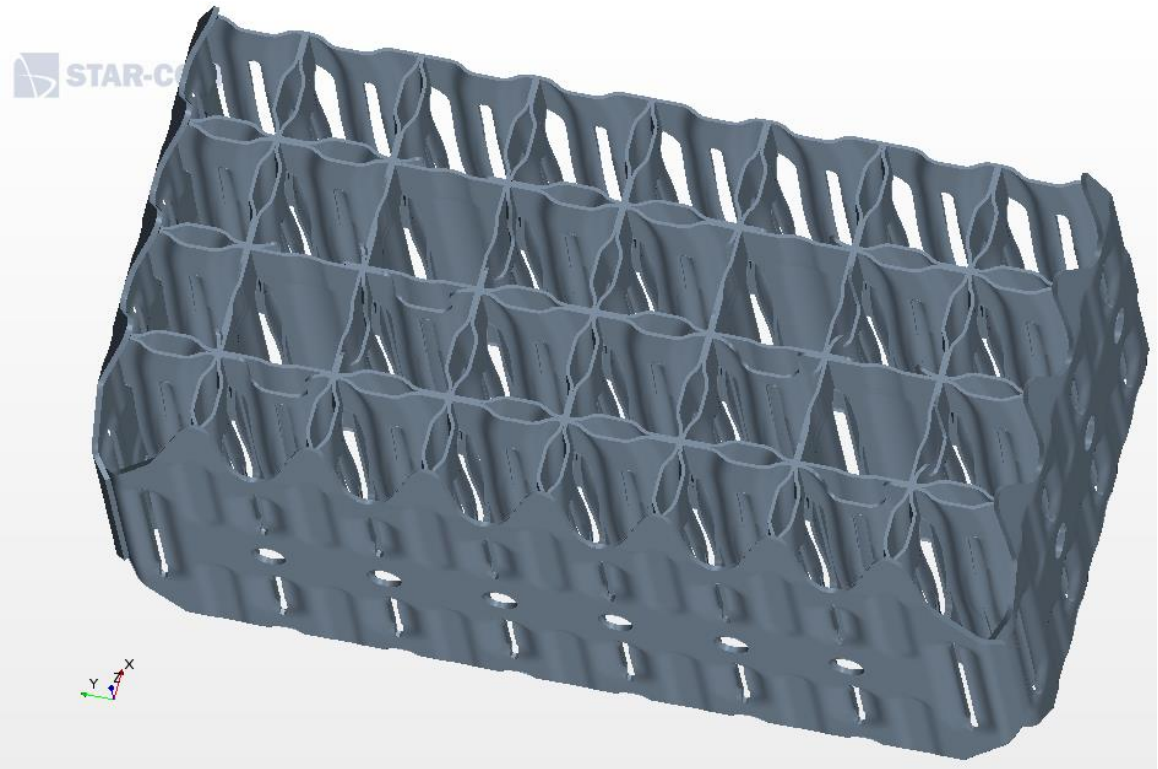

Figure 19: Mechanical beam model and CFD model from side view of HTP 8x8 (FA region: red; Bypass region: blue; SG region= green)

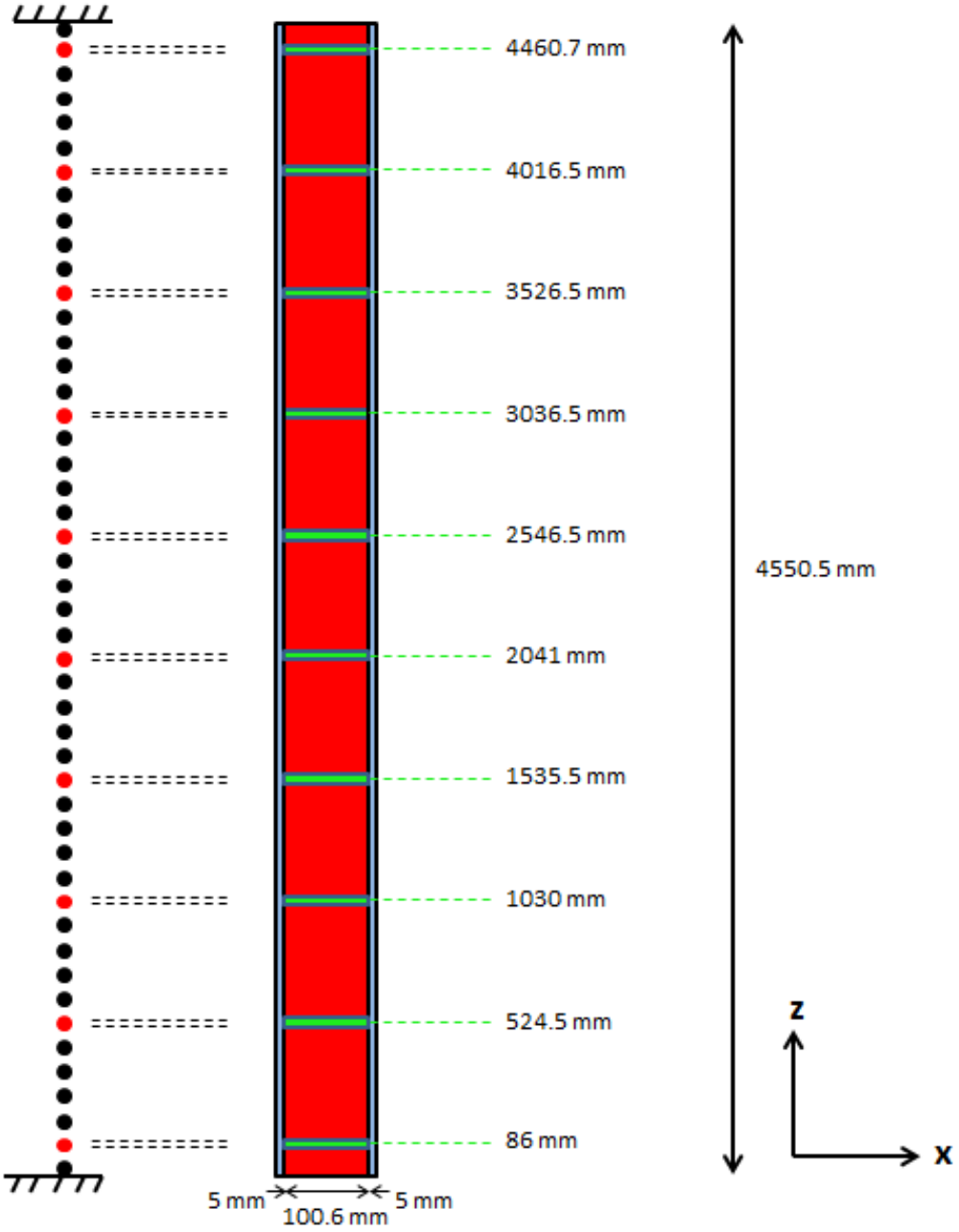

6.2 STRUCTURAL MODEL

For the damping matrix, $\alpha = 1.180\ 10^{-3}$ and $\beta = 1.250$, which correspond to the first and eleven eigenfrequency in air.

The mass of the FA is $M_{st} = 191.0$ Kg. Moreover, the equation for the static FSI is

$$K_{st}.\underline{u} = \underline{F_{fl}} \tag{37}$$

and for the Dynamic FSI simulations

$$M_{st}.\ddot{\underline{u}} + D_{st}.\dot{\underline{u}} + K_{st}.\underline{u} = \underline{F_{fl}} \tag{38}$$

for this case. Time step of

$$\Delta t = 1.10^{-3} s \tag{39}$$

is sufficient to give good results.

6.3 BENCHMARKING OF TURUBULENCE MODEL

In this section, we will first present results of the quasi steady simulation and figure out which of turbulence model is more suitable for our case. And then discuss results of pluck test.

Figure 20: Comparison of the static shape between turbulence model under axial flow (5 m/s).

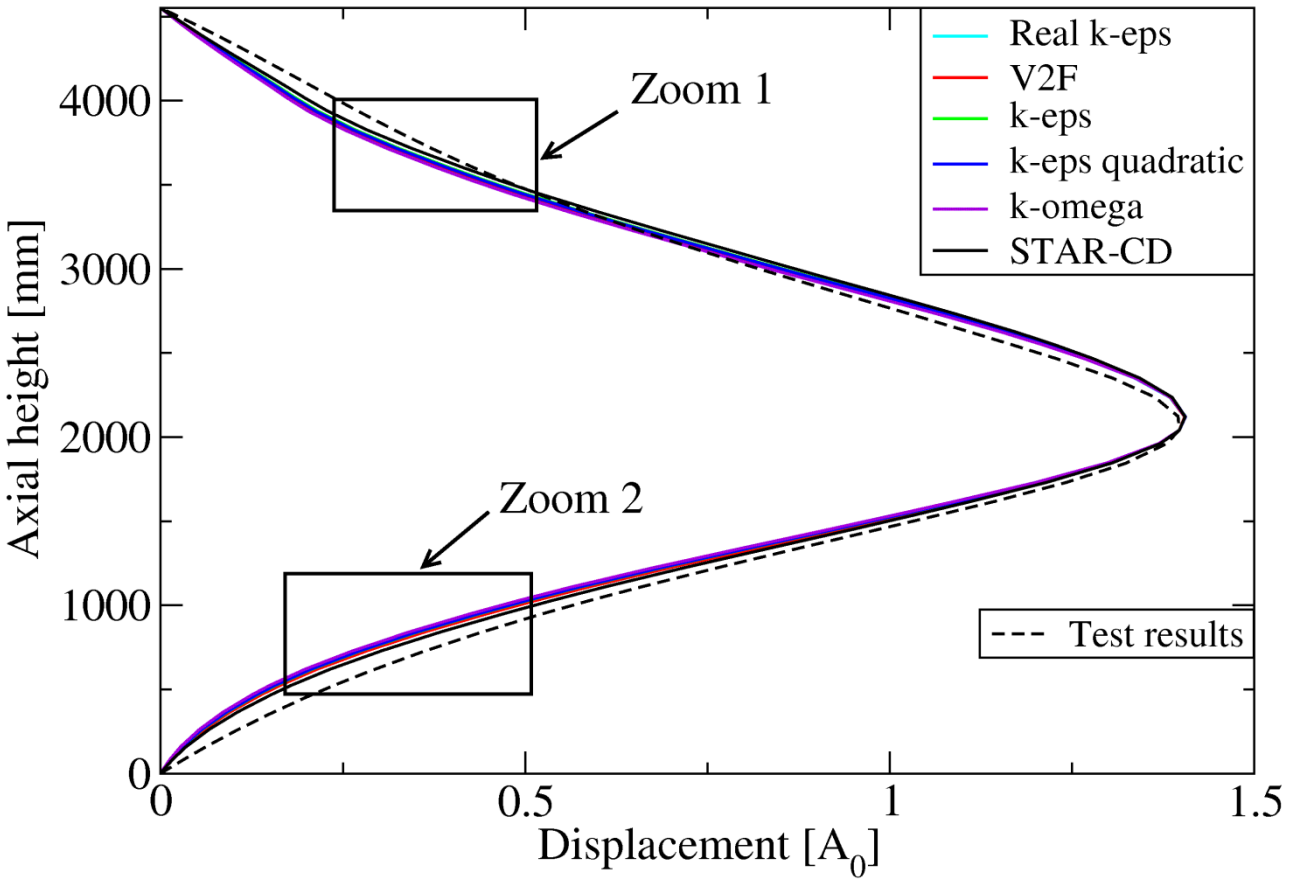

Figure 21: Comparison of the static shape between turbulence model under axial flow (5 m/s) near the top part of the FA (Zoom1).

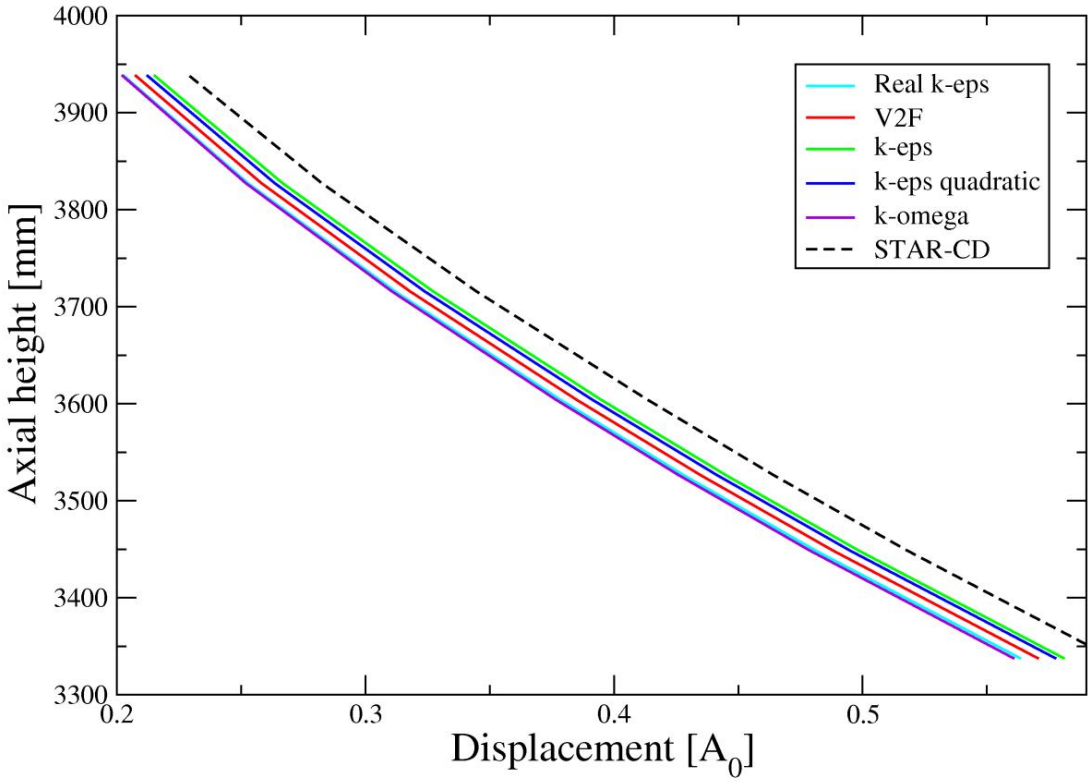

Figure 22: Comparison of the static shape between turbulence model under axial flow (5 m/s) near the bottom part of the FA (Zoom2).

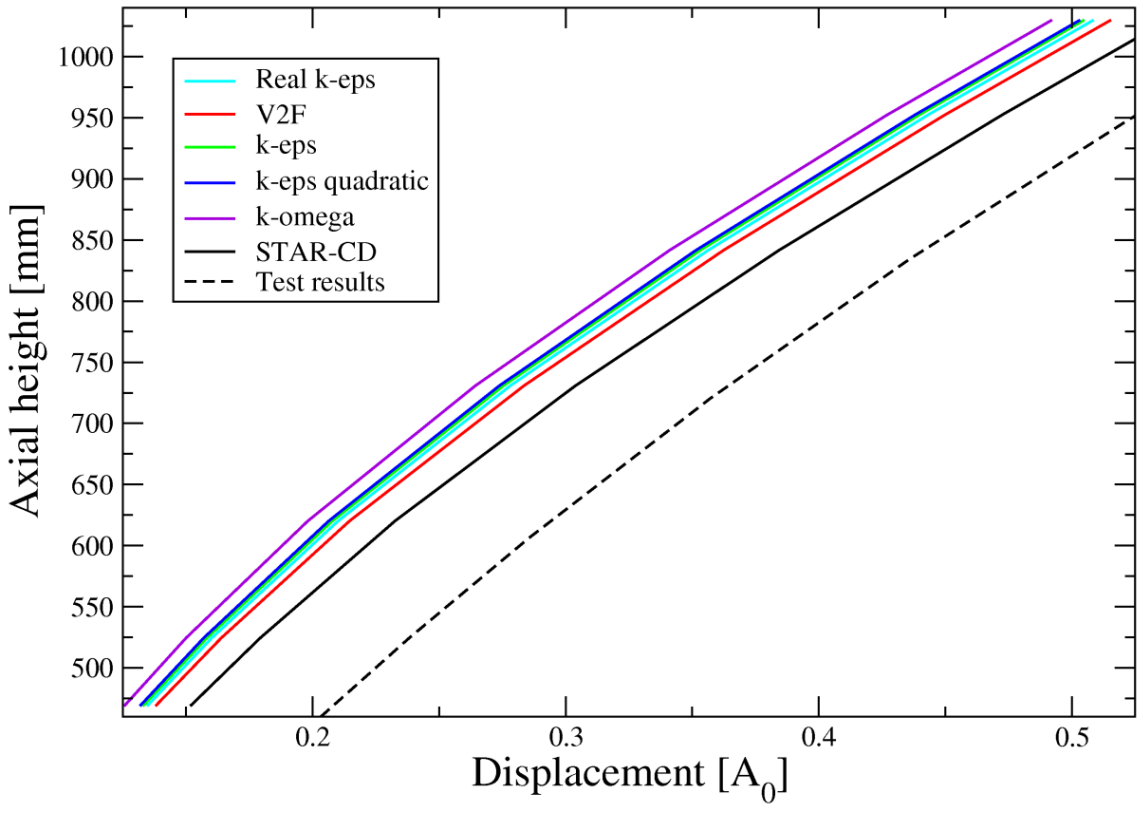

In figure 20, one can easily notice that STAR-CCM+ overestimate the bow of the FA. The fluid force seems to be amplified during the simulation. Figure 21 shows that standard k-eps model gives the best agreement with STAR-CD results regarding the top part of the FA. However, when looking at the bottom part of the FA (see Figure 22), V2F model shows a better accuracy than others turbulence model. If one wants to calculate the gap between the curves in comparison to the results from STAR-CD we find:

- Real k-eps: 3.38 %
- k-eps: 4.39 %
- V2F: 3.48 %
- K-eps quadratic: 3.69 %
- K-omega SST: 5.46 %

Therefore, all turbulence model gives some good results compare to STAR-CD expect for k-omega SST which present the maximum deviation in the bow amplitude of 5.46 %. And prediction from k-omega SST model gives poor results for both top and bottom part of the FA.

Figure 23: comparison of the hydraulic forces of static shape under axial flow (5m/s) between results from FSI coupled CFD simulation STAR-CD and STAR-CCM+.

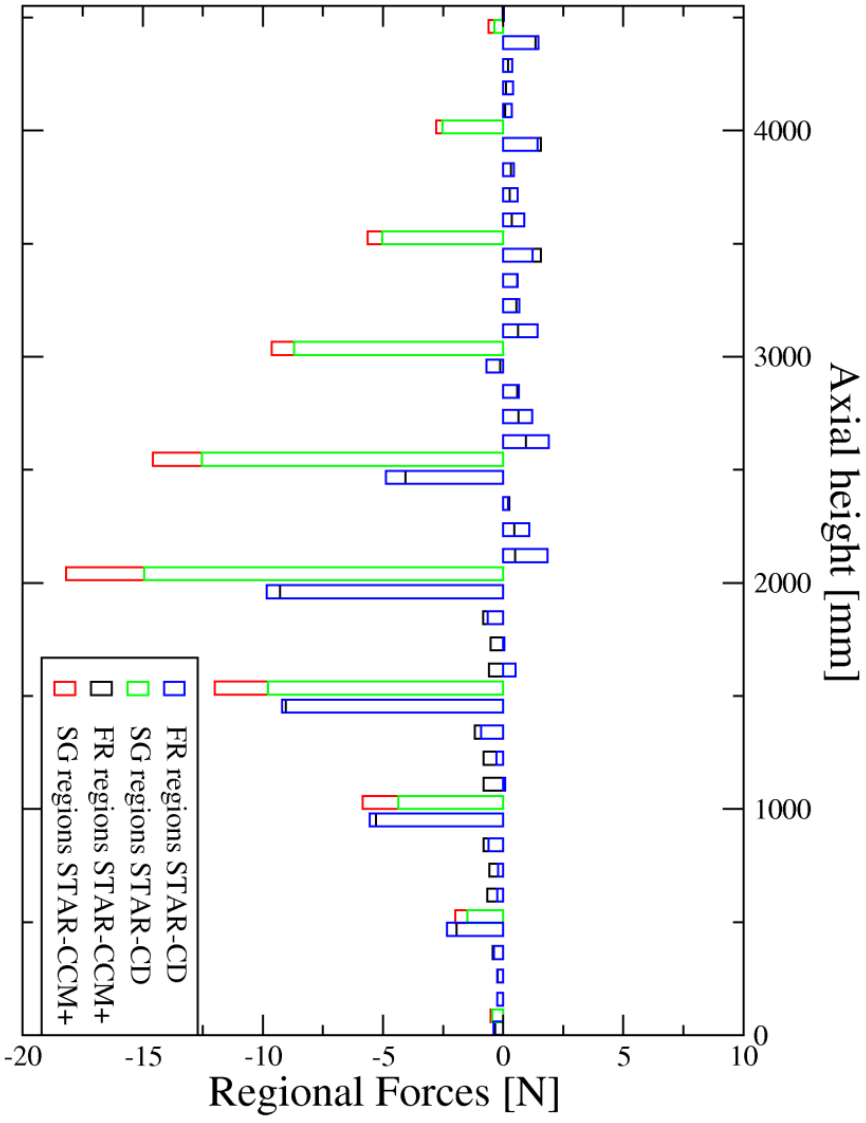

Since the results from STAR-CD gives also an over prediction of the bow shape of the FA regarding to test results, we are seeing that our results move in the wrong direction. One reason can be that in this HTP 8x4 model we have 1 mm gap between the space grids and the wall in regard to the y direction (cf. Figure 17). However, in STAR-CD this gap was set to 1.25 mm. For further investigation of the HTP 8x4 model one could either extend the gap from 1 mm to 1.25 mm in our model or refine the mesh in this area in order to get all the physics effects.

Figure 24: comparison of pluck test with 1.35 A_0 mm initial amplitude at SG5 between test results STAR-CCM+ (Real k-eps) and STAR-CD (Real k-eps).

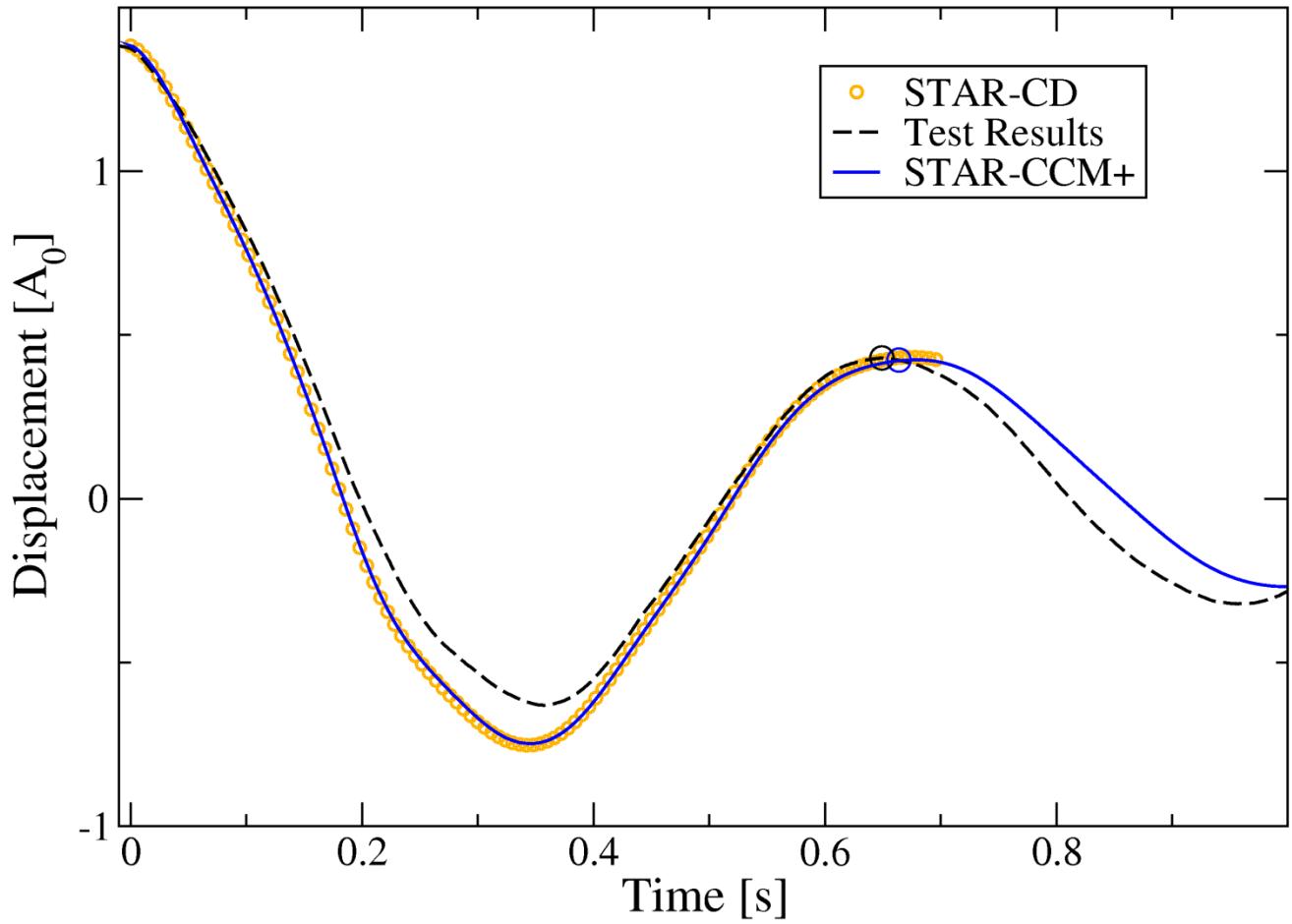

As one can see Figure 23, results from FSI coupled CFD simulation with STAR-CCM+ over predict the force. The total forces at the end of the quasi-steady simulation for the STAR-CD is -79.429 N compare to -98.731 N for STAR-CCM+.

The next step was the determination of response spectrum for pluck tests. Due to lack of time we could only perform this step for three turbulence models. The results show higher damping than expected and also some anisotropy effect. The causes of these phenomenon are under investigation and are good starting point for further study. The first step was to verify if our model was good for pluck test in stagnant water as shown in Figure 24, the results are in a perfect agreement with previous results from STAR-CD. The fact that our simulation doesn't fit perfectly the test results is due to non-linear effect. Indeed, the BALKEN code doesn't take into account non-linear effect. Nevertheless, the three curves crossed each other at the first pic of free oscillation which means that we have good results.

7. CONCLUSION AND PERSPECTIVES

In the first part of this study results of an FSI coupled CFD simulation for calculation of the response spectrum of an HTP 15x15 design has been outlined. Damping values and eigenfrequency have been extract from these simulations. We presented how valuable, mainly for sinus-sweep tests, the BALKEN Fortran code reproduced the FSI coupled CFD simulations with the commercial software STAR-CCM+. We were able to show the robustness of our model by means of a sensitivity study. There is non-linear effect between damping and velocity, therefore it would be interesting to reproduce these pluck tests and sinus-sweep tests with a non-linear code. A code able to capture these effects are under development, hence we will be able to test it in a near future.

In the second part of this study an HTP 8x8 model has been introduced. The methodology for calculation of the eigenfrequency and damping values has been presented. We have seen that the realizable k-eps turbulence model gives the best results regarding the static behavior. The results from pluck tests were not shown in this study but suggest that taking only the half of the fuel assembly has impact on the results. In order to confirm this, a simulation with the whole model (HTP 8x8) could be run but would be extremely time consuming (≈ 400 million cells). Such simulation inevitably takes long time; hence we strongly encourage to work on HTP 8x4 and try to get rid of these anisotropic effect by working on this 1 mm bypass.